THE UNIVERSITY OF MICHIGAN

INDUSTRY PROGRAM OF THE COLLEGE OF ENGINEERING

THE MEASUREMENT OF THE IONIC HALL EFFECT IN SODIUM CHLORIDE

Philip L. Read

A dissertation submitted in partial fulfillment
of the requirements for the degree of
Doctor of Philosophy in the
University of Michigan
1960

November, 1960

IP-473

Doctoral Committee:

Professor Ernst Katz, Chairman
Professor Otto Laporte
Professor William C. Parkinson
Associate Professor C. Wilbur Peters
Professor Edgar F. Westrum, Jr.

ACKNOWLEDGEMENTS

The author would like to express his sincere appreciation to Professor E. Katz for his guidance and assistance during the course of this research. His gentle but penetrating criticism of the various phases of this work was most stimulating.

The author also wishes to thank Professors W. C. Parkinson, G. Weinreich, and J. H. Enns, and Dr. W. Tantraporn for helpful discussions.

The patience and encouragement of the author's wife, Ann, during this work and her invaluable assistance in the preparation of the manuscript are gratefully acknowledged.

The appreciation of the author is also extended to the Industry Program of the College of Engineering for the reproduction of this thesis.

This research was supported by a contract of the United States Navy Department through the Office of Naval Research.

TABLE OF CONTENTS

LIST OF TABLES

LIST OF ILLUSTRATIONS

LIST OF ILLUSTRATIONS - continued

CHAPTER I

INTRODUCTION

1. Introductory Comments

The primary aim of this investigation is the measurement at high temperatures of the mobility of the ionic charge carriers in a single crystal of a pure ionic conductor by subjecting the crystal to crossed electric and magnetic fields and measuring the resulting Hall voltage. This aim is threefold, for it implies: (1) the demonstration of the existence of the ionic Hall effect, which has not previously been observed in a solid, (2) the development of a theory of the ionic Hall effect to relate the measured Hall voltage to the Hall mobilities of the ionic charge carriers, and (3) the measurement of the Hall mobilities over a range of temperatures lying just below the melting point of the material.

The pure ionic conductors studied in this work are sodium chloride and silver chloride in the form of large single crystals. A pure ionic conductor is one in which the conduction of electricity takes place exclusively by means of the transport of ions through the lattice; i.e., where the contribution of electronic charge transport to the total electric conduction is negligible. The crystals which we use are also pure in the sense that they contain no deliberately added impurities.

Sodium chloride and silver chloride are chosen for study because they are examples of the two types of pure ionic conductors in which the expected Hall voltage is relatively high. At high temperatures the ionic conduction in sodium chloride is attributed to the motion of Schottky defects while the conduction in silver chloride is attributed to the motion of Frenkel defects[1].

This work is a continuation of the research of J. L. Levy[2,3] in the general area of ionic conductivity in solids, which was carried out in this laboratory in the early 1950's. Levy set an upper limit for the magnitude of the ionic Hall effect and thereby an upper limit for the difference in the Hall mobilities of the two ionic charge carriers in sodium chloride.

The reasons underlying our attempt to measure ionic charge carrier mobilities at high temperatures are several. In the first place, there exist only a few measurements of charge carrier mobilities in pure ionic conductors[4]. The methods used in making these measurements involve several assumptions about details of processes taking place in the crystal lattice, and the results of these measurements depend critically upon the validity of these assumptions. The measurements have in general not included tests for the validity of the assumptions since such tests are difficult to carry out.

Secondly, when more than one measurement of the ionic mobilities in a given material have been made, the results of these measurements are not in good agreement even though the same method has been

used[4]. It should be pointed out that any measurement of ionic mobilities will be extremely difficult, as is evinced by the small number of such measurements, and thus one would not expect that the agreement among the results be very good.

Nevertheless it is desirable to try to measure ionic mobilities using a method which would be less dependent upon auxiliary assumptions about the nature of processes occurring in the crystal. If this more direct method of measurement were to yield fairly consistent and accurate results, it would act as a check on the validity of the assumptions used and on the validity of the results of these previous measurements.

Moreover, there are no measurements of the ionic mobilities in NaCl or AgCl at temperatures near the melting point of the crystals[4]. The high temperature region is of interest since, with the high thermal energies available, there may be substantial contributions to the conductivity from more than one type of carrier. By using a method which is suitable for high temperature measurements, we had hoped to identify the various types of charge carriers in motion at these high temperatures and measure the mobility of each carrier as a function of temperature.

This work originated in an attempt to repeat and extend the results of Levy; i.e., to measure or to set a lower limit on the size of the ionic Hall effect in sodium chloride. A true ionic Hall effect measurement would represent the first such observation in a solid ionic conductor.

The measurement of the mobilities of ionic charge carriers in a crystal is quite difficult by any method. This difficulty results from the fact that the ionic mobilities are numerically small, on the order of 10^{-8} $(\text{meter})^2/\text{volt-second}$ under the most favorable circumstances[4]. Thus any effect which is sensitive to the magnitude of these mobilities will be correspondingly small. This implies the use of sophisticated procedures and sensitive apparatus in making such measurements.

As might be expected, the mobilities of ionic charge carriers are much lower than electronic mobilities. According to the Bloch[5] description of the motion of electrons in a solid, the conduction electrons may move freely through the lattice, impeded only by the thermal, chemical, and geometrical imperfection of the lattice[6]. On the other hand, ions move through the lattice with difficulty. They are able to move only into a neighboring ion-vacancy site or a neighboring interstitial site[1,7]. The motion of ions involves transporting a relatively large mass compared to that of electrons, and this motion also requires large energies to distort the lattice sufficiently to allow the ion to change lattice sites[7,8,9].

2. Measurement of Ionic Mobilities

It has been only in recent years that a relatively clear understanding of the motion of the ionic charge carriers in a solid has existed, and there are many points which still remain unclear[7]. This understanding might be considered to have started with Ioffe's[10] suggestions in 1923, followed by the defect models proposed by Frenkel[11]

in 1926 and Schottky[12] in 1935. The main reason for this late development of a model for ionic conduction is that measurements of the parameters of ionic charge carriers are generally hard to make. The first reliable measurements of the mobility of the ionic charge carriers in a solid became possible in 1937 with the development of the impurity doping method of Koch and Wagner[13]. However, up to the present time relatively few ionic conductors have been investigated by this method, even though it has remained the most reliable method for estimating carrier mobilities.

There has also recently been a measurement of ionic mobilities in Cu_2O by a special method which, however, is applicable only to that material[14].

The method of Koch and Wagner is based on the observation that if the density of an ionic charge carrier could be increased in an artificial manner, then a measurement of this density increase plus a measurement of the change in the conductivity resulting from this density increase would yield a value for the mobility of the carrier. This observation comes from considering the equation for the conductivity in the case where there is one dominant type of charge carrier, which is given by Equation 2.6

$$\sigma = n\mu q \ , \qquad (1.1)$$

where σ is the conductivity of the crystal, n is the density of the dominant charge carrier, μ is the mobility of this carrier, and q is

its charge. For a known change in the density Δn, a measurable change in the conductivity $\Delta\sigma$ occurs, and the mobility of the carrier is given by

$$\mu = \frac{1}{q} \frac{\Delta\sigma}{\Delta n} \quad . \tag{1.2}$$

The increase in the density of the ionic charge carrier is accomplished experimentally by adding a salt containing aliovalent* impurity ions to the melt from which the crystals are grown. The impurity ions, when incorporated into the crystal lattice, create new lattice defects of the Schottky or Frenkel type[7]. Since the ionic charge carriers are identified with these defects, the addition of the impurity ions effectively increases the carrier density. By controlling the amount of the aliovalent impurity ions in the melt, it is possible to roughly control the increase in carrier density. However, since the concentration of impurity ions in the grown crystal is much less than that in the melt from which the crystal was grown, the crystal must be analyzed to determine the impurity ion concentration. Since the impurity ion concentrations may be extremely small, this analysis constitutes the major experimental problem in the use of this method[15].

---

* An aliovalent impurity ion is one which has a different charge from the host ion which it replaces.

It is necessary to assume in the Koch and Wagner type experiment that the impurity salt enters substitutionally into the lattice in a dispersed fashion, and that it does not form a separate phase in the crystal. Impurity ions belonging to a separate phase will not create additional lattice defects[7]. If a separate phase exists, the relationship between the aliovalent ion concentration and the change in the charge carrier density will be unknown. Evidence for the formation of a separate phase of the impurity salt has been given by Zückler in potassium chloride[16]. Also, the time dependence of the conductivity observed by Etzel and Maurer[17] in their mobility measurements on sodium chloride suggests that a separate phase of the impurity salt was being formed. Thus, even though it is possible to measure the concentration of the aliovalent impurity ions in the crystal, one cannot be sure that all of the impurity ions actually create lattice defects. Tests for the substitutionality of the impurity ions by means of density measurements such as those of Pick and Weber[18] rarely accompany the Koch and Wagner type mobility measurements, although such measurements are useful in setting upper limits for the allowable concentration of impurity ions which will still form a substitutional solution in the lattice.

A second assumption made in the Koch and Wagner method is that the warping of the crystal lattice due to the presence of the impurity ion does not affect the conductivity. Some warping is to be

expected since the ionic size of the impurity ion will not match the size of the normal ion. Any change in conductivity due to this warping must be subtracted from the total change in conductivity due to the presence of the additional charge carriers if one is to make an accurate mobility measurement. The effect of the warping is usually minimized by the choice of an impurity ion which has about the same radius as the normal ion, but the effect is still noticeable[17]. There also exists a lattice distortion due to the charge misfit of the impurity ion, which exists even though the added charge is partially neutralized by the presence of a nearby vacancy. The effect on the conductivity of this charge misfit is more serious[7] than that of the size misfit and requires additional experiments for its determination[19].

A third assumption which is often made is that the lattice defects created by the aliovalent impurity ions have the same ability to act as charge carriers as the thermally created defects previously existing in the lattice. This assumption has been found to be invalid[7,15] even at very low impurity concentrations since the created defects remain bound to the impurity ions with a fairly large energy. A theory of the association of the artificially created defects and the impurity ions has been developed by Stasiw and Teltow[20] and refined by Lidiard[7] and others. This theory includes both the short and long range electrostatic attraction between the impurity and defect and accounts in a rough way for the observed data. The theory does not as yet consider

the association due to the fact that the presence of the vacancy near the impurity ion tends to relieve the local stresses in the lattice due to the misfit of the impurity ion.

One difficulty in the application of the theory is that the association between the aliovalent ions and the artificially created defects is extremely hard to detect. The usual tests for its presence are often not sufficiently sensitive, and separate measurements are required to measure the association over the range of temperatures and impurity concentrations used. Such experiments are rare, and if performed, enhance the complexity of the total Koch and Wagner measurements.

The association of the artificially created defects with the impurity ions prevents them from having the freedom of motion of a thermally created defect. If the results of the Koch and Wagner measurements are not corrected for this association, the calculated mobilities will be somewhat low by an amount varying with the temperature.

To summarize, the method of Koch and Wagner for the measurement of the mobility of ionic charge carriers is not a simple experiment. It involves several assumptions about the introduction of the impurity ions into the lattice and the effect of these impurity ions on the defects which they create. The testing of each of these assumptions generally requires a separate experiment. It is not surprising that the measurements made by this method by two or more investigators on the same material are only in rough agreement.

3. Hall Effect Mobility Measurements

We would like to measure the mobilities of the ionic charge carriers in a pure ionic conductor by a more straightforward method. A natural choice for this method is the measurement of the Hall effect which is widely used to determine electronic mobilities.

The Hall voltage is, in the case of one dominant carrier, directly proportional to the Hall mobility of the carrier. In the case where more than one type of mobile charge carrier is present, the Hall voltage may be interpreted so as to yield the mobility of each carrier type, if the mobilities are sufficiently unequal and if the Hall measurement is sufficiently precise (see Chapter III). The ability to measure in one experiment the mobilities of more than one carrier type is not shared by the Koch and Wagner method. In the Koch and Wagner method the attributes of a selected type of charge carrier are deliberately enhanced so that the attributes of this one carrier type may be studied.

It should be noted here that the Hall mobility of a charge carrier is not necessarily the same as the drift mobility of the carrier since the experimental conditions under which they are measured are different. We shall consider the relation between these two types of mobilities in Chapter III.

There are several advantages to using the Hall effect for mobility measurements. First, the measurement is not dependent upon assumptions about the details of processes occurring in the crystal. Thus we may avoid most of the problems implicit in the Koch and Wagner

procedure. Also, the measurement is sensitive to the sign of the carrier and thus gives additional information about the conduction mechanism under study. The measurement process is non-destructive so that many determinations may be taken on the same crystal with a subsequent benefit to the accuracy of the results. In addition, one expects that the Hall measurements would be most easily performed at high temperatures where the ionic mobilities are high.

The main drawback of the use of the Hall effect as a means of measuring mobilities of ionic charge carriers is that since the mobilities are so low, the Hall voltages are correspondingly small. In fact, the Hall effect in a pure ionic conductor has apparently never been observed[2,21,22]. This is due not so much to the smallness of the effect, for it could be detected with sensitive equipment. It is rather due to the fact that, as noted in Chapter IV, there are always several other transverse voltages which appear across the crystal, voltages which may be many times larger than the Hall voltage. The existence of these large competing transverse voltages makes the observation of the Hall effect, to say the least, difficult.

We would expect this problem to be especially severe in the high temperature range. At high sample temperatures there is a large amount of thermal energy available not only for moving the ions but also for the enhancement of other processes which may take place in the crystal. Furthermore, the high resistance of ionic conductors combined with the high temperatures which we shall be using means that thermal noise will be high.

In essence there are three principal requirements connected with any attempt to use the Hall effect as a means of measuring ionic mobilities in solids. First, the Hall measurement should be made in such a way that the competing transverse voltages are automatically eliminated. Second, the measurement should separate the Hall voltage from any other signals picked up by the Hall probes. Third, the measurement apparatus should be sufficiently sensitive to measure the very low Hall voltages and still maintain a good signal-to-noise ratio. Of course, the experiment must be designed so that there are sufficient checks to make sure that it is really the Hall voltage which is being measured.

The first published attempt to use the Hall effect as a means of measuring the mobilities of ionic charge carriers in a solid was made by Levy[2,3] who tried to measure the Hall mobility of the carriers in NaCl as a function of the temperature in the range 650° to 795°C. He made a thorough analysis of the various types of Hall measurements and was able to design his experiment so as to satisfy the first two requirements listed above. By careful design and construction of his apparatus he was also able to meet the third requirement. However, he was prevented from observing a coherent Hall signal by the presence of a large amount of noise in the sample. These noise voltages were intimately associated with the primary current in the sample but did not seem to have the characteristics of the usual kind of current noise.

Levy was unable to detect Hall signals smaller than the noise level since he had only a short time interval in which to make a measurement at any given temperature. However, if any Hall signal were present, it was certainly less than the observed noise voltage. This set an upper limit for the Hall voltage over the temperature range in which he worked and also set an upper limit for the difference in the Hall mobilities of the sodium ion and chlorine ion vacancies in this region.

The upper limits which Levy set on the Hall voltage in NaCl were of the same order of magnitude as the expected Hall voltage which he calculated on the basis of the mobility results of Etzel and Maurer[17] and the transport number data of Tubandt et al.[23]. Thus, it was of great interest to try to repeat Levy's Hall measurements on NaCl with the hope of reducing the effect of the current noise so that the actual Hall signals might be detected. It was also of interest to attempt Hall measurements on an ionic conductor of the Frenkel defect type.

In line with the suggestions put forth in Levy's dissertation, Hall effect apparatus of greater sensitivity was designed and built. This was done in the hope of reducing the effect of the perturbing current noise by the use of weaker applied electric fields. Also, the apparatus was designed so that Hall measurements could be taken over relatively long time intervals and this data recorded automatically. In this way it was hoped that the current noise could be averaged out over the time interval of the measurement. All possible sources of noise exterior to the sample itself were carefully eliminated.

In order to make meaningful measurements over long time intervals, the equipment had to be made much more stable, the effects of vibrations and other perturbing effects on the equipment had to be reduced, and the environment of the sample had to be maintained in a more constant mechanical, thermal, and electrical state.

The secondary aim of this investigation is the design and construction of apparatus of the necessary sensitivity, stability, and accuracy to allow us to make more precise measurements of the Hall effect than did Levy.

4. Choice of Ionic Conductors Studied

Sodium chloride is perhaps the best known example of an ionic conductor and as such has received much experimental and theoretical attention. It is logical that we should use it in our study of ionic conductivity. However, there may be other pure ionic conductors which would be more favorably suited for making Hall measurements.

Accordingly, the known pure ionic conducting materials were surveyed. In order that a material have the largest Hall effect, there should be a maximum numerical difference between the mobility of the major (more mobile) and of the minor ionic charge carriers over the temperature range of interest. This condition arises from the fact that the average Lorentz force on both the major and minor charge carriers is in the same direction. Also, it is not possible to separate the temperature variation of the mobility of the two carriers

from the Hall voltage data unless there is a high major to minor carrier mobility ratio. Other criteria relate to the commercial availability of the material or its ease of preparation, the number of phases in which it exists, sensitivity to external fields, decomposition at high temperatures, etc.

The results of this survey showed that among Schottky defect ionic conductors sodium chloride offered the best chance for the measurement of the Hall effect. The drift mobility of the sodium ion vacancy at the melting point of NaCl is higher than the drift mobility of the carriers in any of the other Schottky defect conductors in which measurements have been made. Little information is available on the mobilities of the minor carriers in these materials. Large single crystals of quite pure sodium chloride are commercially available, and the material is easy to handle. All of this, plus the fact that we would like to repeat Levy's measurements on NaCl, led to the use of NaCl in our work.

In the class of Frenkel defect ionic conductors, silver chloride seemed to be the best choice, in spite of its sensitivity to light. The high numerical difference in the carrier mobilities in AgCl renders it an attractive candidate for Hall effect studies.

CHAPTER II

IONIC CONDUCTIVITY

1. Definitions

In this section we shall briefly define the quantities involved in the description of ionic charge transport in solids.

Let us consider a simply-connected, homogeneous region of a solid in which there are no temperature gradients. If we subject this region to an externally applied electric field, there will in general be set up within the region an electric current of density J. In a crystal lattice of cubic symmetry, the quasi-equilibrium situation which is set up after all transient effects associated with the establishment of the current in the region have vanished is described by Ohm's law

$$J_i = \sigma E_i \ , \tag{2.1}$$

over a wide range of applied electric field strengths E. Here, σ is the conductivity of the material. In our work we shall always be dealing with cubic crystals and low electric field strengths, so that Equation 2.1 is valid. We shall also use alternating fields whose frequency is sufficiently high that polarization effects may be neglected.

Now, the current density due to any type of charge carrier is the product of the density, average velocity, and charge of that carrier; and the total current density is the sum of this product over all types of mobile carriers.

Let us consider a single type of carrier of charge q. Under conditions of no applied electric field it is possible to define a density of carriers n which will be uniform throughout the region. Upon application of the electric field, the crystal will no longer be in an equilibrium situation, and the density of carriers may be changed and may also be a function of position within the region. However, in ionic conductors the charge carrier density is virtually undisturbed by the application of the electric field. Thus we may restrict our attention to the situation where the application of the field does not change the equilibrium density of carriers and where the distribution remains uniform throughout the region.

It should be mentioned that there are various possible ways of defining the density of ionic charge carriers in a solid. For example, if carriers may exist in either a trapped or mobile state, one may include in n at any instant either the total number of carriers or only the untrapped ones. We shall always follow the former convention.

The i component of the average velocity of the type of charge carrier which we are considering is defined by

$$< v_i > = \frac{1}{n} \sum_{s=1}^{n} (v_i)_s \ , \qquad (2.2)$$

where $(v_i)_s$ is the i component of the velocity of each individual

carrier. In ionic conductors the only motions of the charge carriers which contribute to this sum are those from one lattice or interstitial site to a neighboring site. The velocity of the motion of the carrier as it oscillates about its equilibrium position is not considered, since it does not contribute to the net motion of the carriers.

With no applied electric field, the velocities of the jumping carriers are distributed so that there is no net transport of charge in any direction. This does not, however, imply that the velocities are randomly oriented, because there may be preferred directions of motion. On application of the electric field the equilibrium distribution of the velocities is not preserved since there is a net flow of charge. The average velocity of this net charge transport, where the average is taken over all of the carriers n, is called the average drift velocity of this type of carrier.

The average drift velocity of a carrier type is proportional to the first power of the electric field strength over the range of validity of Equation 2.1 and is given by

$$\langle v_i \rangle = \mu E_i . \tag{2.3}$$

The proportionality coefficient μ is called the drift mobility of the carrier type.

The total current density is given by

$$J_i = \left(\sum_r q_r n_r \mu_r\right) E_i , \tag{2.4}$$

where the sum is over the r types of mobile charge carrier present in the region of the solid. From Equation 2.1 we may write the conductivity as

$$\sigma = \sum_r q_r \, n_r \, \mu_r \quad . \tag{2.5}$$

The partial conductivity σ_p due to the motion of the carriers of type p is

$$\sigma_p = q_p \, n_p \, \mu_p \quad . \tag{2.6}$$

In this connection it is convenient to define the transport number of a charge carrier type. The transport number t of a carrier type is the fraction of the total current which is transported by that carrier type. The transport number t_p of the pth carrier type is

$$t_p \equiv \frac{\sigma_p}{\sigma} \equiv \frac{q_p \, n_p \, \mu_p}{\sum_r q_r \, n_r \, \mu_r} \quad . \tag{2.7}$$

In the ionic conductors with which we shall be working there are only two carrier types which have equal density and equal charge (of opposite sign). Here, the ratio of the transport numbers of the two carriers is

$$\frac{t_a}{t_b} = \left| \frac{\mu_a}{\mu_b} \right| \quad . \tag{2.8}$$

2. Charge Transport in Ionic Conductors

Aside from the fact that all pure ionic conductors must (by definition) obey Faraday's law and also that ionic conductors obey

Ohm's law up to extremely high electric field strengths, the main experimental characteristic of these materials is the rather striking temperature dependence which their conductivity exhibits[24]. We shall, in this section, describe the models which have been proposed to account for the occurrence of a finite conductivity and which explain the temperature dependence of the conductivity in ionic conductors.

The conductivity of an ionic conductor increases rapidly with temperature but there are two regions in which the rate of increase is somewhat different. On a log σ versus $1/T$ plot, where T is the absolute temperature, this increase is represented by two almost[15] straight lines of different slope in the high and low temperature regions joined together by a curve in a transition region. The transition curve may be smooth or it may exhibit a more complicated structure[7]. The transition temperature is dependent upon the history of the sample. If a normal crystal is purified by recrystalization or other means, the transition region will occur at a lower temperature. However, if aliovalent impurities are added to a normal crystal, the transition region occurs at a higher temperature[25]. In both cases the conductivity at any temperature in the low temperature region seems to decrease or increase in direct proportion to the amount of aliovalent impurity removed from or added to the crystal, whereas the high temperature conductivity is unaffected.

The existence of the observed conductivity in single crystals of pure ionic conductors is attributed to the presence of a small number of thermally and chemically created imperfections in the lattice structure.

Without these deviations from the perfect crystalline array of ions in the crystal, it is difficult to account for the magnitude of the ionic conductivity. In a perfect lattice the only possible conduction process which could take place and at the same time preserve the perfection of the crystal would be a succession of interchanges of neighboring anions and cations[7]. However, in NaCl one anion-cation interchange would require an increase in the electrostatic energy of the ions of about 15 ev. On this basis extremely high electric fields (on the order of 10^8 v/cm) would be required to observe a measurable ionic charge transport, whereas experimentally one can observe an ionic current with applied fields of only a few v/cm.

It is also evident that the imperfections in the crystal lattice are not created by the applied field[26]. From the fact that the conductivity increases rapidly with temperature, we might guess that the imperfections in the lattice have a thermal origin, or at least that thermal creation will be the dominant factor at high temperatures. The presence of aliovalent impurities in the crystal must also have a role in the creation of lattice defects, especially at low temperatures. Other possible sources for the creation of imperfection in the lattice are geometrical imperfections caused by externally applied stresses and defects caused by subjecting the crystal to high energy radiation. However, in a well-annealed crystal isolated from external stress and radiation fields these sources of defects are relatively unimportant.

The creation of lattice defects by the incorporation of aliovalent impurity ions into the crystal lattice during the growth of the crystal is a well-known process and explains the behavior of the low temperature portion of the conductivity plot[7]. However, since we shall be concerned only with the high temperature region of conductivity, we shall consider only the thermal creation of defects, which is the dominant source at these temperatures.

Two types of thermally created lattice disorder, Frenkel[11] and Schottky[12] disorder, have been proposed to account for the observed high temperature conductivity in pure ionic conductors and these models have been supported by much experimental work in the last thirty years. Frenkel disorder in an otherwise perfect lattice is created when an ion is removed from its normal lattice site and is fitted into an interstice in the lattice. Frenkel disorder thus consists of the presence of two types of lattice defects, one being the interstitial ions and the other being the vacant lattice sites. The existence of each of these defects makes possible a net motion of ions through the crystal when an electric field is applied since both the interstitials and the vacancies may move. It is apparent that the number of interstitials will be equal to the number of vacancies in Frenkel disorder. Even though the density of the interstitials and vacancies are equal, their mobilities may be somewhat different, so that they may contribute to the total charge transport in different amounts; i.e., they may have different transport numbers.

The vacancy is able to move through the lattice by virtue of the fact that neighboring ions (of the same kind as the ion which formerly occupied the vacant site) may jump into the vacancy. The motion of the vacancy is opposite to that of the jumping ion, which gives the vacancy an effective charge opposite to that of the jumping ions. The interstitial ions were formerly thought to move through the lattice by jumping directly from one interstitial position to the next. But it is now thought that the motion takes place by the interstitialcy mechanism[7,27,28]. This involves the original interstitial ion pushing a neighboring ion (of the same kind) from its normal lattice site into an interstitial position, while the original interstitial then occupies the site of the evicted ion. The interstitialcy mechanism is probably energetically more favorable than the direct motion through the interstitial lattice in the case of AgCl[28].

The energy necessary to move an interstitial ion or vacancy is only a small fraction of the energy necessary for anion-cation interchange and is typically about 0.5 ev[4]. This is consistent with the magnitude of the observed conductivity in ionic conductors.

Although many ions participate in the motion of both the vacancy and the interstitial, the identity of the defects is maintained through many jumps. For this reason the role of charge carrier is usually assigned to the defects and the motion of the individual ions is ignored.

Schottky disorder in the lattice is created when anions and cations are removed from the interior of the lattice and placed in normal sites on a surface (external or internal) of the crystal. Schottky disorder thus consists of cation vacancies and anion vacancies. The presence of these vacancies allows a net motion of ions through the lattice when an electric field is applied. Once again, the role of charge carrier is assigned to the vacancies since they maintain their identity as they move through the crystal.

The vacancies are created in a definite ratio depending on the valences of the anion and cation. In a salt of the type AB the density of anion vacancies will be equal to that of the cation vacancies. The mobilities of the two types of vacancy are usually quite different because of the difference in their ionic size.

The question of which type of disorder, Frenkel or Schottky, will occur in a given material is determined by such parameters as the ratio of the ionic sizes of the cation and the anion, the strength of overlap repulsive forces, the van der Waal's forces between the ions, etc.[1,7]. In NaCl experimental evidence indicates that only Schottky disorder is present, even at high temperatures, while in AgCl the predominant disorder is the Frenkel type with perhaps a small contribution from Schottky disorder near the melting point[29].

A simple theory of the mobility of ionic charge carriers in a single crystal of an ionic conductor has been developed by Wert[30] and elaborated by Lidiard[7]. In the case of a cubic crystal of the

NaCl type, under no external pressure, where only one type of mobile charge carrier is present, the mobility of that carrier is given by

$$\mu = \frac{1}{T}\left[\frac{q\nu}{k}\sum_i (d_i \cos\varphi_i)^2 \; e^{\frac{S_a}{k}}\right] e^{-\frac{U_a}{kT}}, \qquad (2.9)$$

where T is the absolute temperature, q is the charge of the carrier, k is Boltzman's constant, ν is the frequency of vibration of the carrier in its potential well (in a possible jump direction), S_a is the entropy of activation, U_a is the activation energy evaluated at $T=0°$, d is the distance of a jump, φ is the angle between the jump direction and the applied electric field, and where the sum is taken over all possible forward (in the direction of the applied electric field) jump directions.

In the case of both NaCl and AgCl, this is given by

$$\mu = \frac{1}{T}\left[\frac{q\nu a^2}{k} \; e^{\frac{S_a}{k}}\right] e^{-\frac{U_a}{kT}} = \frac{A}{T} \; e^{-\frac{U_a}{kT}}, \qquad (2.10)$$

where a is the lattice constant. The pre-exponential coefficient is denoted by A.

In both NaCl and AgCl at the high temperatures at which we shall be working, there are two types of mobile ionic charge carriers present. The mobility of each carrier will be given by an equation of the form of Equation 2.10. The contribution of each carrier to

the conductivity will be additive. However, the Hall fields produced by the two types of charge carriers will oppose each other, since the Lorentz force on both types of carrier will tend to drive them toward the same side of the crystal. Thus the contributions of the two types of mobile charge carriers to the production of the Hall voltage are subtractive.

The entropy of activation which appears in Equation 2.10 has been estimated by consideration of the effect of the motion of the defect on the normal vibrational modes of the lattice[31,32,33]. The entropy factor is estimated to be on the order of magnitude of 10^0-10^1.

3. Mobility Measurements in NaCl

It should first be remarked that NaCl is a pure ionic conductor under the conditions of our experiments. Chemically pure NaCl in stoichiometric balance and in the absence of strong electromagnetic fields, electron or neutron bombardment, or excess alkali or halide vapor, exhibits no measurable electronic conductivity even at temperatures very close to the melting point[2]. The addition of impurities in small amounts does not change the nature of the conductivity[7]. The fact that NaCl is a pure ionic conductor has been demonstrated directly over a wide range of temperatures by the electrolysis measurements of Tubandt et al.[23].

The negligible electronic conduction in NaCl is not unexpected since the forbidden band width is about 9.6 ev, as estimated from measurements of the ultraviolet absorption maximum[34]. This implies

that at the melting point of NaCl only one electron in 10^{45} will have sufficient thermal energy to be raised from the valence band into the conduction band. Of course, there may be bound donor states for electrons associated with crystal defects which lie two or three ev below the bottom of the conduction band[35,36]. However, in the absence of energetic radiation almost all of the electrons will be closely associated with the sodium or chlorine ions and there will be extremely few electrons available to populate these bound states.

There are in the literature two measurements of the drift mobility of the sodium ion vacancies in single crystals of NaCl, both being Koch and Wagner type measurements. The first measurement was made by Etzel and Maurer[17] in 1950 using cadmium chloride as the impurity salt. Bean[15] in 1952 extended these measurements over a wider temperature range using calcium chloride as the impurity salt.

The results of the mobility measurements of Etzel and Maurer made in the temperature range 256-403°C are given by

$$\mu = \frac{1.96}{T} e^{-\frac{9860}{T}} \frac{(\text{meter})^2}{\text{volt-sec.}} \quad . \tag{2.11}$$

Etzel and Maurer used the association theory of Stasiw and Teltow[20] to interpret their data.

The data of Etzel and Maurer has been reanalyzed by Lidiard using his refined association theory[37]. The corrected value for the

mobility of the sodium ion vacancies given by Lidiard is

$$\mu = \frac{2.12}{T} e^{-\frac{9750}{T}} \frac{(\text{meter})^2}{\text{volt-sec.}} . \qquad (2.12)$$

Bean worked in the temperature range from 160-680°C and found a mobility at high temperatures, where associated effects were low[7], of

$$\mu = \frac{0.46}{T} e^{-\frac{9050}{T}} \frac{(\text{meter})^2}{\text{volt-sec.}} . \qquad (2.13)$$

This result differs somewhat from those given by Equations 2.11 and 2.12.

Both of these previous measurements are subject to all of the problems implicit in the Koch and Wagner method listed in Chapter I. This would seem to account for the divergence in the results of the two experiments.

The activation energies and the pre-exponential coefficients found in these two measurements are tabulated in Table I. Although these are the only mobility measurements on the cation vacancies in NaCl, it is possible to infer values for the activation energy of the sodium ion vacancies in NaCl from low temperature conductivity measurements. The values of U_a found from the low temperature conductivity measurements of Etzel and Maurer[17], Lehfeldt[24], Smekal[38], Mapother et al.[39], and Phipps et al.[40], are given in Table I for comparison with the values derived from mobility measurements. Also given are values of U_a inferred from the low temperature diffusion

TABLE I

VALUES OF THE ACTIVATION ENERGY AND THE PRE-EXPONENTIAL COEFFICIENT IN THE MOBILITY EXPRESSION FOR SODIUM ION VACANCIES IN NaCl

Measurement or Calculation	Activation Energy ev	Pre-exponential Coefficient $(meter)^2 - °K/volt\text{-}sec.$
Mobility Measurements:		
Etzel and Maurer	0.85	1.96
Etzel and Maurer/Lidiard	0.84	2.12
Bean	0.78	0.46
Conductivity Measurements:		
Etzel and Maurer	0.85	
Lehfeldt	0.78	
Smekal	0.89	
Mapother et al.	0.83	
Phipps et al.	0.88	
Other Measurements:		
Mapother et al. (diffusion)	0.77	
Rief (resonance)	0.66	
Nowick and Dreyfus (quenching)	0.75	
Calculations:		
Mott and Littleton	0.51	
Dryden and Meakins	0.54	
Guccione et al.	0.87	

measurement of Mapother et al.[39], the resonance experiment of Rief[41], and the quenching experiments of Nowick and Dreyfus[42]. These additional experimental determinations of U_a are in the same range as the values found by the mobility experiments.

Three theoretical determinations of the activation energy of the sodium ion vacancies in NaCl have been made, and are listed in Table I. These are the calculations of Mott and Littleton[8], Dryden and Meakins[43], and Guccione et al.[9]. The work of Guccione et al. is considered to be the most accurate calculation, and it agrees fairly well with the experimental values.

Theoretical determinations of the pre-exponential coefficient must await the development of a more refined mobility theory. The simple theory gives values which are about a factor of ten lower than the experimental values.

Although there are no measurements of the mobility of the chlorine ion vacancies in NaCl, it is possible to estimate this mobility. In the diffusion measurements of Laurent and Benard[44] the diffusion coefficients of both ions in NaCl were measured over the temperature range from 600-800°C. Under the assumption that at the high temperatures used the Nernst-Einstein relation[7] is valid in the diffusion process of both ions, the diffusion coefficient D for each ion is proportional to the partial conductivity due to that ion, and by Equation 2.7

$$\frac{D_{Cl^-}}{D_{Na^+}} = \frac{t_-}{t_+} .$$

Using their measured values for the diffusion coefficients, the ratio of the transport numbers is

$$r = \frac{t_-}{t_+} = 2.20 \times 10^2 \, e^{\frac{-7300}{T}} . \qquad (2.14)$$

This is plotted in Figure 1.

For comparison we have also plotted in Figure 1 Levy's extrapolation[2] of Tubandt's transport number measurements[23] which gives for r the value

$$r = 1.90 \times 10^3 \, e^{-\frac{9100}{T}} . \qquad (2.15)$$

The two determinations of the transport number ratio are in fair agreement.

We may use the transport number ratio in Equation 2.14 to calculate an expression for the mobility of the chlorine ion in NaCl. By Equation 2.8 the mobility of the chlorine ion may be found from either of the sodium ion vacancy mobility measurements. If, for example, we use Lidiard's corrected mobility data Equation 2.12, the mobility of the chlorine ion will be

$$\mu_{Cl^-} = \frac{4.66 \times 10^2}{T} \, e^{-\frac{17,050}{T}} . \qquad (2.16)$$

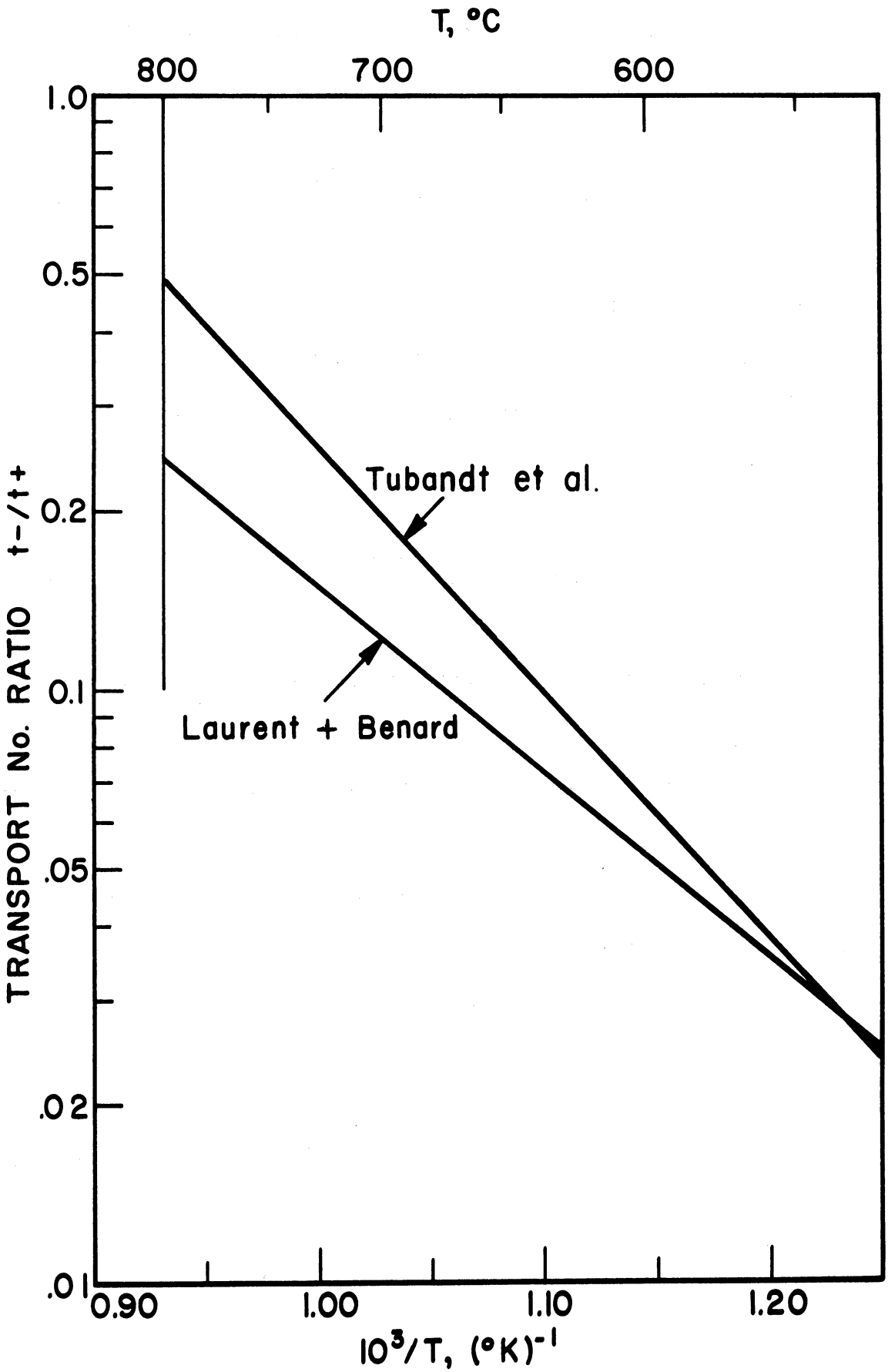

Figure 1. Transport Number Ratio in NaCl

This is plotted in Figure 2 along with the mobility of the sodium ion vacancies from Equation 2.12. We have also drawn in this graph the difference in the carrier mobilities of the two ion vacancies, since this difference is what will be measured by our Hall measurements (see Chapter III). We have listed in Table II the parameters appearing in Equation 2.16 and also the values of the activation energy for the motion of the chlorine ion vacancies calculated by Mott and Littleton[8], Dryden and Meakins[43], and Guccione et al.[9]. Again, the last calculation is the most accurate.

TABLE II

VALUES OF THE ACTIVATION ENERGY AND THE PRE-EXPONENTIAL COEFFICIENT IN THE MOBILITY EXPRESSION FOR CHLORINE ION VACANCIES IN NaCl

Calculation	Activation Energy ev	Pre-exponential Coefficient $(meter)^2$-°K/volt-sec.
Equation 2.16	1.48	4.66×10^2
Mott and Littleton	0.56	
Dryden and Meakins	1.80	
Guccione et al.	1.11	

It should be mentioned that recent measurements by Barr et al.[45] on the diffusion of the chlorine ion vacancies in NaCl

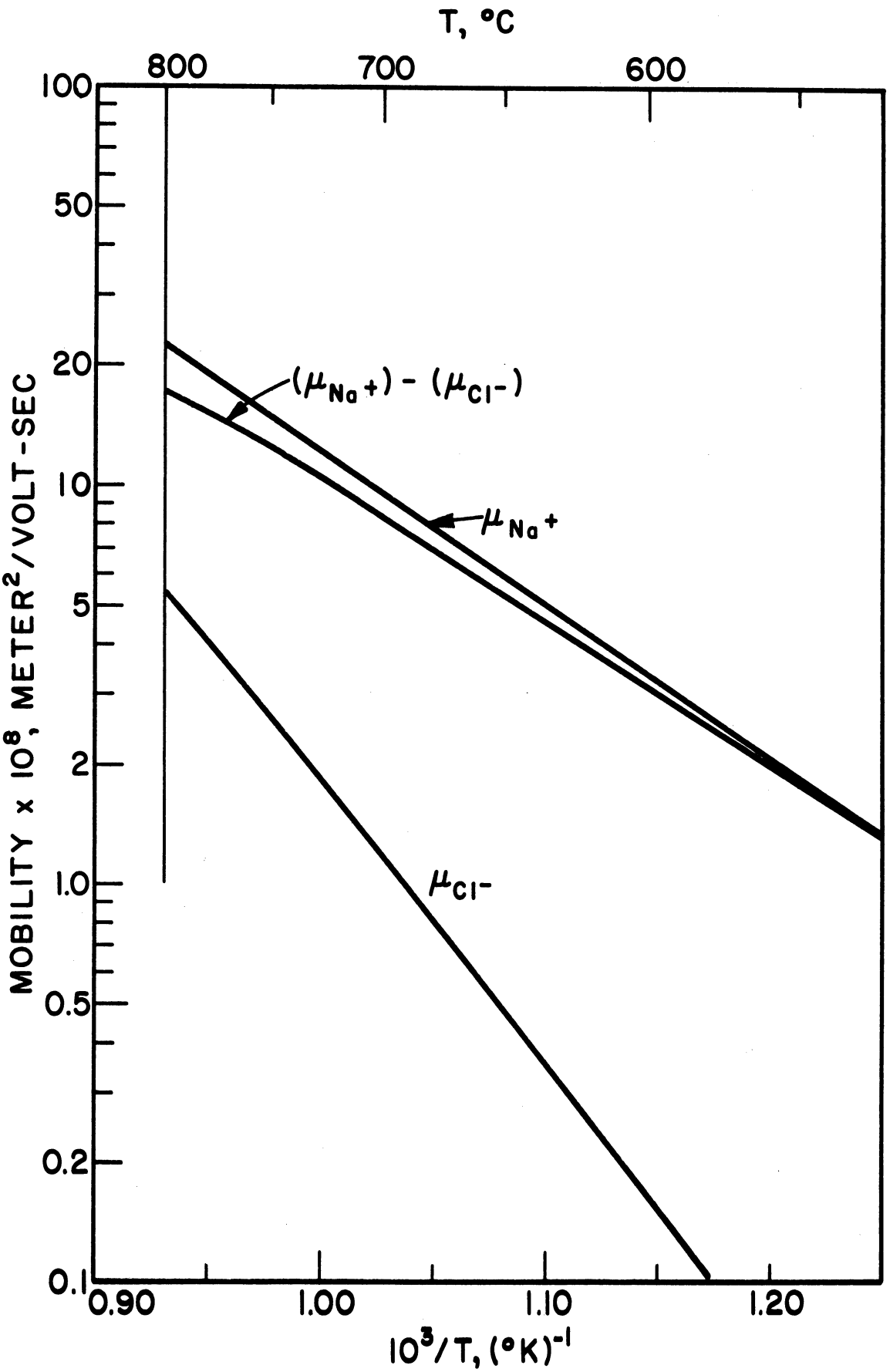

Figure 2. Difference of Drift Mobilities of the Ionic Charge Carriers in NaCl.

have shown that the diffusion coefficient is very sensitive to the presence of gross imperfections such as dislocation lines. Thus, our estimate of the mobility of the chlorine ion vacancies must be considered to be very approximate. We are, however, only interested in an order of magnitude estimate of this mobility.

4. Mobility Measurements in AgCl

Since we attempted Hall effect measurements in AgCl as well as in NaCl, we shall briefly summarize the previous drift mobility measurements of the ionic charge carriers in AgCl.

Two measurements of the drift mobility of the silver ion vacancies and interstitials in AgCl have been made. The first was the classic experiment of Koch and Wagner[13]. In their experiment they assumed that the mobilities of the silver vacancies and interstitials were equal, and they also implicity assumed that the association between the artificially created carriers and the aliovalent impurity ions was zero. Thus, their results are somewhat unrealistic.

The second measurement was made by Ebert and Teltow[29] in 1955. After correcting for association effects, they arrived at the results plotted in Figure 3. The difference in the mobilities of the two carriers is somewhat higher than in NaCl.

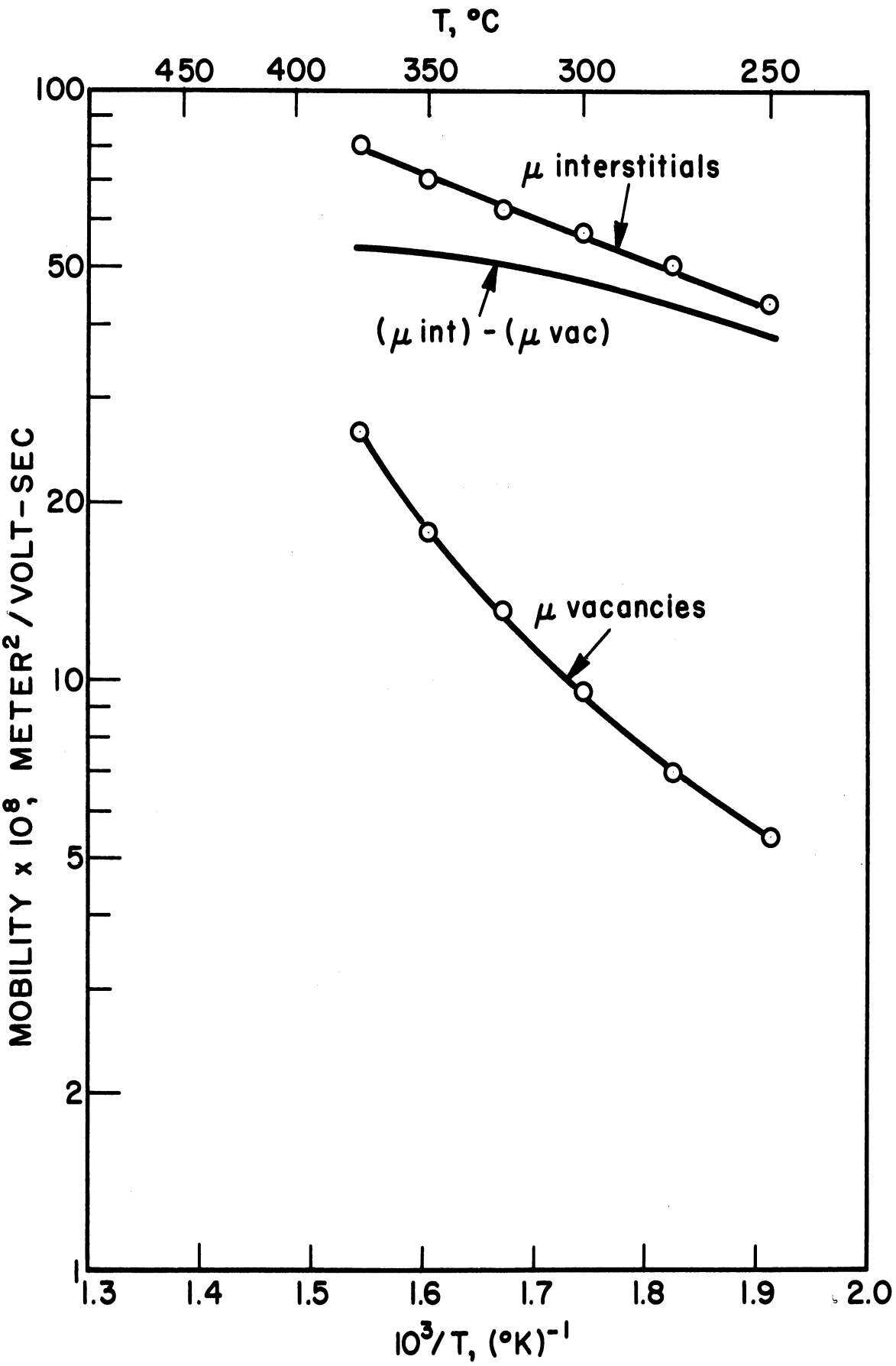

Figure 3. Drift Mobility Measurements in AgCl.

CHAPTER III

THEORY OF THE HALL EFFECT IN AN IONIC CONDUCTOR

1. Introduction

We have proposed the use of Hall effect measurements as a means of measuring the mobilities of the ionic charge carriers in a pure ionic conductor. In order to interpret our Hall voltage measurements in terms of the carrier mobilities, we must possess a theory of the Hall effect in ionic conductors.

A simple theory of the Hall effect in ionic conductors has been given by Levy[2], but this theory does not explain the origin of the ionic Hall effect. It seems desirable to develop a theory which is based on the physical picture of the conduction process in ionic conductors and which explicitly demonstrates the processes leading to a non-zero Hall effect.

In the development of this theory it is necessary to re-examine the usual mobility theory for ionic conduction and note that, among the possible refinements of this theory, there is one small correction term which should be included. Starting from this corrected mobility theory we shall develop a theory for the ionic Hall effect in which the physical basis of the effect will be evident.

The theory of the Hall effect relates the Hall mobilities of the ionic charge carriers to the measured Hall voltage. Since the previous measurements of the carrier mobilities in ionic conductors

have measured the drift mobilities of the carrier, it is also desirable to consider the relationship between the two types of mobilities, so that we may compare the results of our Hall mobility measurements with these drift mobility measurements.

The results of the theory will then be specialized for use in our situation in which ac applied fields are used, two types of charge carrier are present, and square samples are used.

2. Re-examination of the Usual Mobility Theory

The results of the usual theory[7,30] of the mobility of ionic charge carriers in an ionic conductor given in Chapter II are substantially correct. However, there are several possible refinements of the mobility theory which might be made, each leading to a small correction term. We shall consider here only one such refinement which is necessary for the development of the theory of the Hall effect in ionic conductors.

Ionic charge carriers are usually pictured as moving in a potential energy well which has high (~15 ev) walls in most directions but which has in these walls in a few directions gaps which present a relatively low (~0.5 ev) barrier to the motion of the carriers. The low portions of the energy barrier have a saddle point configuration[26]. The shape and width of the gap near the saddle points may well have an effect on the motion of the carriers, but these features would be a function of the particular material under consideration. Thus, we shall ignore any such effects, just as is done in the usual mobility theory.

The carriers will oscillate about their equilibrium position in the well since they are thermally excited by the vibrations of the lattice. The energy distribution of the carriers is given by a Maxwell-Boltzman distribution, since quantum effects may be ignored. The basis of the usual mobility theory is the assertion that the probability per second that an ionic charge carrier will jump from one site to a neighboring one over a given barrier is equal to[7,30]

$$P_j = N\, e^{-\frac{G_a}{kT}}, \tag{3.1}$$

where N is the number of approaches per second which the carrier makes to the barrier, and where G_a is the Gibbs free energy associated with the barrier. Equation 3.1 may be expressed in the form

$$P_j = N\, M\, e^{-\frac{U_a}{kT}}, \tag{3.2}$$

where U_a is the (activation) energy associated with the barrier and where M represents a factor containing the entropy of activation (volume of activation factor drops out since pressure is almost zero).

The usual theory is developed essentially one dimensionally. That is, the only motions of the carrier which are considered are those in a possible jump direction. This means that all carriers which have an energy greater than U_a will be able to make a jump. Consideration of a two- or three-dimensional lattice shows that this model is somewhat unrealistic, for possible motions of an energetic ($U > U_a$) carrier

exist where no jump could take place. However, for simplicity, we shall continue to assume that the motions of the charge carriers in their potential well are such that all carriers moving in the general direction of a saddle point will pass through the saddle point (jump) if they have an energy greater than U_a.

It will greatly simplify the development of the theory and also will make more evident the essential features of what follows if we introduce a specific geometry for the ionic conductor at this point. The basic structure of the theory is independent of the model adopted and applies equally well to other situations.

Let us then consider a two-dimensional lattice of cubic symmetry which is of the NaCl type. Let us choose the direction of the electric field which is to be applied so that it coincides with one of the cubic axes. Also let us consider that only one type of carrier, an ion vacancy, is present. There will be four possible jump directions for the carrier. If the electric field direction represents the reference (0°) angle of a polar coordinate system whose origin is at the center of the potential well, then the possible jump directions are in the neighborhood of 45°, 135°, 225°, and 315°. Let us denote these jump directions by I, II, III, and IV according to the quadrant number.

Under no applied fields, the net ionic current in a crystal must be zero, once an equilibrium situation is established. (We shall always assume that no temperature gradients exist in the crystal.)

The net jump probability summed over all possible jump directions must also be zero. By the symmetry of the crystal, both the activation energy and the number of approaches per second to the barrier are the same in all jump directions. The factor M depends on the lattice and is independent of the jump direction. If we denote the value of N under no applied fields by N_o, and the activation energy by U_o, then the jump probability in any direction is

$$P_o = N_o M e^{-\frac{U_o}{kT}} . \tag{3.3}$$

If we now apply an electric field $\vec{E}$ to the crystal, the average energy required of the carriers to be able to pass over one of the saddle points is no longer equal in all of the jump directions. Also, the number of approaches per second which are made to the barriers by the carriers is modified by the electric field. This latter effect is not considered in the usual mobility theory and is the correction which we wish to emphasize.

The energy which is required to pass over a saddle point is changed by the electric field in the amount of

$$\Delta U = q (\vec{E} \cdot \vec{s}) , \tag{3.4}$$

where q is the charge of the carrier and $\vec{s}$ is the distance directed from the center of the energy well to the saddle point. The height of the energy barriers in the forward (in the direction of $\vec{E}$) direction

is lowered and the height of the backward energy barriers is raised. In our case the forward energy barriers are lowered by $qEa/4$, where a is the lattice constant. The backward energy barriers are raised by the same amount. The asymmetry of the jump energy requirements leads to a net motion of carriers in the forward direction.

It is clear that the average number of approaches per second which the carriers make to the saddle points will also be affected by the electric field. In the forward jumping directions there will be an increased number of carriers per second whose direction of motion is not reversed by the energy barrier, since there is an increased number of jumps per second over the lowered barriers. On the other hand, in the backward jumping directions there will be an increased number of carriers per second whose direction of motion is reversed by the barrier, since the barrier height is raised by the electric field. As a result, at any time there will be more carriers moving in the forward direction than in the backward direction in the potential well, although this difference is small.

Let us denote the increase in the number of approaches per second which the carriers make toward a forward saddle point by ΔN. The decrease in the number of approaches per second made toward a backward saddle point will also be equal to ΔN. Thus, under the influence of an applied electric field the probability per second of a

jump in a forward direction will be given by

$$P_{for}\,|_{E} = (N_o + \Delta N)\, M\, e^{-\left(\frac{U_o - \Delta N}{kT}\right)}, \qquad (3.5)$$

and in a backward direction by

$$P_{back}\,|_{E} = (N_o - \Delta N)\, M\, e^{-\left(\frac{U_o + \Delta U}{kT}\right)}. \qquad (3.6)$$

The net jump probability per second in the longitudinal direction will be

$$P_{\text{net long}}\,|_{E} = \sum_{for} (P_{for}|_{E}) - \sum_{back} (P_{back}|_{E}), \qquad (3.7)$$

where the sums are over the possible forward and backward jump directions. In our case this is

$$P_{\text{net long}}\,|_{E} = 4M\, e^{-\frac{U_o}{kT}} \left(N_o \sinh \frac{\Delta U}{kT} + \Delta N \cosh \frac{\Delta U}{kT}\right). \qquad (3.8)$$

Since the arguments of the sinh and cosh are always very small at the temperatures of interest, Equation 3.8 becomes

$$P_{\text{net long}}\,|_{E} = \frac{4M\, N_o\, \Delta U}{kT}\, e^{-\frac{U_o}{kT}} \left(1 + \frac{\Delta N\, kT}{N_o\, \Delta U}\right). \qquad (3.9)$$

The first term of this expression is just the result of the usual mobility theory, and the second term is a small correction term.

The quantity ΔN may be calculated by considering that it is directly related to the net current in a given direction. Thus

$$\Delta N = (P_{for}\,|_{E} - P_o) - (P_{back}\,|_{E} - P_o) \,. \tag{3.10}$$

Substitution of Equations 3.3, 3.5, and 3.6 into Equation 3.10 yields an equation for ΔN. Neglecting $\exp(-U_o/kT)$ with respect to 1, the solution for ΔN is given by

$$\Delta N = \frac{2N_o\,\Delta U}{kT}\; e^{-\frac{U_o}{kT}} \,. \tag{3.11}$$

Substituting this value for ΔN into Equation 3.9

$$P_{net\ long}\,|_{E} = \frac{4M\,N_o\,\Delta U}{kT}\, e^{-\frac{U_o}{kT}} \left(1 + 2e^{-\frac{U_o}{kT}}\right) . \tag{3.12}$$

This shows that the correction term is indeed small; for NaCl at $T = T_{melt.\ pt.}$ it is on the order of 10^{-4} of the leading term.

3. Theory of the Hall Effect

Next, let us consider the effect of an applied magnetic field on the net jump probability per second. In our special geometry, the magnetic field is applied in a direction perpendicular to the plane of the two-dimensional lattice.

The effect of the magnetic field, when there is no applied electric field present, is to change the paths of motion of the charge carriers as they oscillate in the potential well. The magnetic field, however, has no effect on the shape of the potential well or the height of the energy barriers. The new paths taken by the charge carriers will be slightly more curved than their former paths as dictated by the Lorentz force on each carrier. Some carriers whose motion had originally carried them into the neighborhood of one saddle point will now be curved into the neighborhood of an adjacent saddle point. The symmetry of the situation guarantees that the number of carriers per second deflected away from any given saddle point toward other saddle points will be equal to the number of carriers per second deflected away from other saddle points toward the given saddle point. Therefore, when no external electric field is present, the application of a magnetic field does not on the average disturb the equilibrium situation and the net jump probability per second will remain zero.

Let us now consider the situation where both a magnetic field $\vec{B}$ and an electric field $\vec{E}$ are applied to our two-dimensional crystal. The height of the energy barriers is affected by the electric field but not by the magnetic field. The magnetic field will, however, affect the number of carriers per second which approach the various saddle points.

The number of carriers per second deflected away from the region of a given saddle point toward an adjacent saddle point will be a function of: (1) the magnetic flux density B, (2) the number of carriers per second which initially approach the given saddle point, and (3) the velocity distribution of these carriers. Now, presumably the velocity distribution of the carriers, which is established by thermal excitation, will be the same in all directions. Thus, the asymmetry in the number of carriers per second which are deflected away from the region of a saddle point will be the same as the asymmetry in the number of approaches per second initially made (with no magnetic field) toward the saddle point. The number of carriers per second deflected away from a given saddle point is

$$\text{No. per second deflected} = FN^*B, \tag{3.13}$$

where N^* is the number of carriers per second which approach the saddle point with no magnetic field and where F is the fraction of carriers per unit magnetic flux density which are deflected away from the region of the saddle point.

Let us consider the case of a magnetic field which is directed so that the Lorentz force on the carriers moving toward saddle point I deflects some of them toward saddle point II, and deflects some of the carriers originally moving toward saddle point II toward saddle point III, etc. The number of carriers per second

deflected away from saddle point I will be $F(N_o+\Delta N)B$ and the number of carriers per second deflected toward saddle point I will also be $F(N_o+\Delta N)B$. The number of carriers per second deflected away from II will be $F(N_o-\Delta N)B$ whereas the number of carriers per second deflected toward II will be $F(N_o+\Delta N)B$ for a net gain of $2F\Delta NB$. The number of carriers per second deflected both away from and toward III will be $F(N_o-\Delta N)B$. And the number of carriers per second deflected away from IV will be $F(N_o+\Delta N)B$ while the number of carriers per second deflected toward IV will be $F(N_o-\Delta N)B$ for a net loss of $2F\Delta NB$.

The jump probability per second in the various directions will now be

$$
\begin{aligned}
P_I|_{E,B} &= (N_o + \Delta N)\, e^{-\frac{U_o-\Delta U}{kT}}, \\
P_{II}|_{E,B} &= [N_o - (1 - 2FB)\Delta N]\, e^{-\frac{U_o+\Delta U}{kT}}, \\
P_{III}|_{E,B} &= (N_o - \Delta N)\, e^{-\frac{U_o+\Delta U}{kT}}, \\
P_{IV}|_{E,B} &= [N_o + (1 - 2FB)\Delta N]\, e^{-\frac{U_o-\Delta U}{kT}}.
\end{aligned}
\tag{3.14}
$$

If we now evaluate the net jump probability per second in the transverse direction, we find that

$$
P_{\text{net trans}}|_{E,B} = 4\, F\Delta NBM \cosh\frac{\Delta U}{kT}\, e^{-\frac{U_o}{kT}}, \tag{3.15}
$$

which, by the fact that the argument of the cosh is small, is equal to

$$P_{\text{net trans}}\Big|_{E,B} = \frac{8\ FN_0B\Delta UM}{kT}\ e^{-\frac{2U_0}{kT}} . \qquad (3.16)$$

Thus there is a non-zero net jump probability in the transverse direction.

As a result, an ionic current will be established in the transverse direction. In a sample of finite width this current will eventually be neutralized by the establishment of a transverse electric field, the Hall field. This Hall field is the direct result of the action of the applied magnetic field on the directional distribution of N^*.

The net jump probability per second in the longitudinal direction will, after the establishment of the Hall field, be once again given by Equation 3.12. This does not mean that there will be no magnetoresistance effects, but rather that to the first order in B there is no change in the longitudinal current. We have, in our development of this theory, ignored second order path differences in the deflection of the oscillating carriers. In order to obtain higher order terms in both the Hall effect and the longitudinal current, it is necessary to consider explicitly these higher order effects.

The Hall angle Θ_H defined by[46]

$$\Theta_H \approx \tan\Theta_H \equiv \frac{E_{\text{trans}}}{E_{\text{long}}} = \frac{P_{\text{net trans}}\Big|_{E,B}}{P_{\text{net long}}\Big|_{E,B}} , \qquad (3.17)$$

where E_{trans} is the intensity of an electric field which corresponds to the initial transverse current density. This is from Equations 3.12 and 3.16 equal to

$$\Theta_H = 2FB\, e^{-\frac{U_o}{kT}} . \tag{3.18}$$

The Hall field E_H is the negative of E_{trans} and from Equation 3.17 is

$$E_H \equiv -\Theta_H E_{long} ; \tag{3.19}$$

or, since $E_{long} = E$, the applied electric field intensity, this is

$$E_H = -2FBE\, e^{-\frac{U_o}{kT}} . \tag{3.20}$$

The Hall voltage V_H is

$$V_H \equiv -E_H w , \tag{3.21}$$

where w is the width of the sample, or from Equation 3.20

$$V_H = 2FEB\, w\, e^{-\frac{U_o}{kT}} . \tag{3.22}$$

The Hall mobility μ_H is defined by[47]

$$\mu_H \equiv \frac{\Theta_H}{B} , \tag{3.23}$$

and is, from Equation 3.18

$$\mu_H = 2F\, e^{-\frac{U_o}{kT}} . \tag{3.24}$$

The relationship between the Hall mobility and the measured Hall voltage is thus

$$\mu_H = \frac{V_H}{E\, B\, w} , \tag{3.25}$$

in the case of the model which we have considered with only one type of charge carrier present.

In order to generalize our results to a three-dimensional cubic lattice, we have only to take into account the additional jumping directions. This will introduce a factor 2 into Equations 3.8, 3.9, 3.12, 3.15, and 3.16. The expressions for the Hall angle, Hall field, Hall voltage, and Hall mobility are unchanged since they depend on ratios of the altered equations.

The symmetry of the cubic lattice guarantees that the above results hold even though the electric and magnetic fields are not directed along cubic axes, as in our model. The same results will also hold in the case where the ionic charge carrier is an interstitial ion rather than an ion vacancy.

The generalization of this theory to crystal lattices of lower symmetry than that of the cubic lattice may be carried out using the above development as a basis. However, we are here interested only in cubic lattices of the NaCl type.

4. Relationship Between Hall and Drift Mobilities

The Hall mobility given by Equation 3.24 is of the same general form as the drift mobility given by Equation 2.10. An exact comparison of the two mobilities depends on the evaluation of F in the Hall mobility expression. We were unable to perform this evaluation without appealing to special models of the motion of the charge carriers in the potential well.

It is evident, however, that the factor which relates the two mobilities is of the order of magnitude of unity, just as in the electronic case, since the essential difference between the two mobility definitions is in the averaging over the velocities with which the carriers move in the potential well.

5. Application of the Theory to Our Measurements

The above theory has to be slightly modified to fit the particular circumstances of our Hall measurements. We shall be using samples which are of finite length, applied fields which are alternating, and materials in which two charge carriers are mobile. The theory was developed for the case of only one carrier present, and it was implicitly assumed that the samples were of infinite length. Also, the ac character of the applied fields was not taken into account.

The two types of ionic charge carrier which are present in NaCl and AgCl are of equal density and of equal but opposite sign. Each carrier type will have a Hall mobility of the form given by Equation 3.24. As was noted in Chapter II, the Lorentz force of both carrier types will be in the same direction, which implies that the Hall fields set up by the two carrier types will oppose each other. If the mobilities of the two carrier types were equal in magnitude, the net Hall field which would be set up would be zero.

In general, over the entire temperature range of interest, the two types of ionic charge carriers in NaCl and AgCl will have unequal mobilities. Thus, the net Hall field set up by the transverse motion of the two carrier types will be non-zero and will be equal to the difference in the Hall fields of the individual carrier types. The Hall voltage observed in our measurements represents a net Hall mobility which is the difference in the mobility of the major and the minor carrier, and the $\ln \mu_H$ vs. $1/T$ plot will be of the form shown in Figure 2.

If the Hall measurements are sufficiently accurate and are made over a sufficiently broad temperature range, and if the ratio of the mobilities of the two carrier types is high over part of that range, it is in principle possible to determine the temperature dependence of each carrier type from the Hall measurements. The separation is made by following the graphical subtraction technique used in the determination of the half-lives of two radioisotopes which occur

in the same material[48]. A curve is fitted to the apparent Hall mobility data (on a ln $\mu_H T$ vs. 1/T plot) calculated from Equation 3.25. An extrapolation is made from the straight portion of this curve at the low end of the temperature range. The extrapolated straight line represents the mobility of the major carrier, and the difference between the straight line and the curve fitted to the experimental points represents the mobility of the minor carrier.

In the development of the theory we did not consider the effect which the ends of the sample have on the Hall voltage. The fact that the electric field electrodes cover the entire ends of our samples means that no transverse voltage can exist in these regions. The correction for these end effects has been considered by Isenberg et al.[49]. For samples of equal length and width such as we use, the relation between the measured and true Hall voltage is given by

$$V_H(\text{meas.}) = 0.674\ V_H(\text{true})$$

If we insert this into Equation 3.25, we find

$$\mu_H = \frac{V_H(\text{meas})}{0.674\ V\ B}, \tag{3.26}$$

where V is the voltage of the electric field applied across the length of the sample.

If we now consider that the applied fields are alternating and that the values in Equation 3.25 represent rms quantities, then

$$V_{H_{rms}} \text{ (true)} = \frac{\mu_H B_{rms} V_{rms}}{\sqrt{2}} \quad . \tag{3.27}$$

Therefore, the net Hall mobility in our measurements will be, from Equations 3.26 and 3.27

$$\mu_H = \frac{2.10 \, V_{H_{rms}} \text{ (meas)}}{V_{rms} B_{rms}} \quad . \tag{3.28}$$

CHAPTER IV

EXPERIMENTAL APPARATUS AND PROCEDURES

1. Hall Effect Measurement Method

We carefully chose the parameters of our Hall effect measurement in order to optimize our chances for observation of the Hall effect in pure ionic conductors. As a consequence we used the ac cross-modulation[50] type of Hall voltage measurement with applied electric and magnetic fields at 85 cps and 60 cps respectively and with a 25 cps Hall voltage detector. We also chose to use a square sample and the usual four-electrode configuration with one Hall probe grounded.

The experiment was designed to measure the open-circuit Hall voltage across the sample rather than the short-circuit transverse current. This choice was dictated mainly by the high resistance of the samples which limits the Hall currents to the micro-microampere range. The measurement of ac currents of this magnitude presents more extreme experimental problems than does the measurement of the ac open-circuit voltages corresponding to these currents.

An ac Hall effect measurement method was used in order to avoid the problems associated with the preliminary compensation of the initial voltage imbalance in the Hall electrodes, the presence of other transverse voltages due to thermoelectric and thermomagnetic effects, and the polarization of the primary current.

The small size of the expected Hall voltage means that the preliminary compensation (with only the applied electric field present) of a voltage imbalance in the Hall electrodes using a dc method must be on the order of at least one part in 10^7, which is not possible at the high sample temperatures used.

The presence of transverse voltages other than the Hall voltage is assured by the inevitable existence of temperature gradients across the sample[2]. Possible sources of these other transverse voltages are thermomagnetic effects such as the Ettinghausen-Nernst effect, which arises from the presence of a longitudinal temperature gradient, and thermoelectric effects such as the Seebeck effect in the Hall probe circuit, which arises when the Hall probes are at different temperatures (the probes being made of a different material than the sample)[51]. Such temperature gradients exist naturally at the high sample temperatures used and are also created by the Peltier effect in the case of the primary electrodes, and the Righi-Leduc effect and the Ettinghausen effect in the case of the Hall probes[51]. These transverse voltages may be as large as or larger than the Hall voltage.

The presence of small and varying contact potentials between the Hall probes and the sample would also hamper a dc measurement.

If a dc applied electric field were used, the polarization of the primary current would quickly reduce the Hall voltage to zero so that the Hall voltage detection would have to be very fast. It is doubtful whether a sensitive detector with sufficiently fast response could be constructed.

Therefore, it was necessary to use an ac method.

There are several types of ac Hall effect measurements which might be used. Levy[2] made a careful study of the various possibilities and concluded that the ac cross-modulation method was the best choice.

The primary advantage of this method is that the Hall voltage can be chosen to appear at a frequency different from the frequency of either of the applied fields or of their harmonics. If the frequency of the applied electric field is ν_1 and the frequency of the applied magnetic field is ν_2, then the Hall field will appear at the frequencies $(\nu_1 + \nu_2)$ and $(\nu_1 - \nu_2)$. Since, in principle, the Hall voltage detector will respond only at either the sum or difference frequency, the preliminary compensation of the initial voltage imbalance across the Hall probes can be very crude. The amount of compensation is determined by the magnitude of signals which the Hall voltage detector can accept without mixing them; i.e., the linear range of the detector.

The ac cross-modulation method will be free of the problems associated with dc measurements if the frequency of the applied electric field is high compared to the frequency of temperature variations in the sample and also high enough to avoid polarization effects. Our frequencies were so chosen.

The principal practical difficulty in using this method is that extreme caution has to be exercised so that there is no mixing of the signals from the primary fields other than by the Hall effect

in the sample. This means that nonlinear elements in the apparatus must be avoided and that the various portions of the apparatus must be well isolated from each other.

The choice of the frequencies of the applied fields is based on three factors. First, the high resistance of the sample presents a high source impedance to the Hall voltage detector. If the detector is to be isolated from the strong ac magnetic field present in the region of the sample, it will have to be located at some distance from the sample. This requires long connecting wires between the Hall probes and the detector input, wires which must be well shielded against pickup. The capacitance of these wires and the attendant shielding will greatly attenuate the Hall signal unless a low frequency is used for the Hall signal. Second, it is expensive to construct a strong ac magnet at a frequency other than 60 cps. Third, the noise in the input stage of the detector will be due mainly to flicker effect at low audio frequencies, which increases as 1/f, so that a Hall voltage frequency as high as possible should be chosen.

We have followed Levy's suggestions[2] in using a magnetic field at 60 cps, an electric field at 85 cps, and in measuring the 25 cps difference frequency Hall voltage. The choice of a relatively low Hall frequency allows the use of the special techniques which have been developed for ultra-low frequency circuits and which function best at frequencies close to zero cps. This advantage offsets the increased flicker noise at these frequencies and allows a high input impedance for the detector.

The determination of the sample's shape and size depends upon making a compromise between conflicting requirements. As far as the shape of the sample is concerned, we have restricted our attention to right parallelopipeds. This was done because the cleavage planes in NaCl are perpendicular to the cubic axes; consequently, the samples may be most easily prepared in this shape. We felt that it was important to disturb the samples as little as possible from their state as grown, for the mobility of the ions in the crystal may well depend upon the density of dislocations, crystal boundaries, etc., present[45]. The cleaving of the crystals into shape would seem to introduce the least amount of stress in the crystal.

For optimum results the sample size would be rather large. It is desirable to have a wide sample so that the Hall voltage, which is proportional to the width, is also large. It is also desirable to have a large length-to-width ratio so that the end effect[49] reduces the measured Hall voltage as little as possible. However, both the length and the width of the sample are limited by the necessity that the sample be immersed in a uniform magnetic field. The size of the homogeneous field provided by the available ac magnet has limited our sample area to about 7 cm^2.

It was found by Levy that a sample of equal length and width had fewer thermal inhomogeneities than a rectangular sample. Therefore the equipment was designed to accept square samples approximately 2.6 cm on a side. The thickness of the sample is fairly arbitrary as long

as it is well defined, although it is advantageous to use a fairly large thickness to reduce the sample resistance. However, the available space between the pole faces of the magnet set a limit of about 0.2 cm on the possible thickness.

The electrode configuration which we have utilized is the standard four-electrode one, with two electrodes for the application of the applied electric field covering the ends of the sample and the Hall probes being essentially point electrodes on either side of the crystal. Configurations using fewer electrodes would have yielded a smaller Hall voltage, and configurations with more than four electrodes would have increased the electrode contact noise.

We also followed the recommendation of Levy in choosing one of the Hall probes to be at ground potential and in using a balanced (ungrounded) output from the system producing the applied electric field. The grounding of one of the Hall probes simplifies the shielding problem, and it also results in a higher signal-to-noise ratio in the detector. This comes about because the use of a balanced input to the Hall system would have required the use of a back-to-back cathode follower input stage, each half contributing its noise to the signal. It is impossible to use a transformer input because of the danger of mixing of the primary signals in this somewhat nonlinear element.

2. Experimental Apparatus

The following is a description of the apparatus which we used in making ac cross-modulation Hall effect measurements in NaCl and AgCl. Although the equipment was especially designed for samples of these materials, it is also suitable for measurements on other pure ionic conductors, as well as high resistivity electronic conductors.

The apparatus consists of five parts:

1) source of the applied electric field
2) source of the applied magnetic field
3) Hall voltage measurement system
4) sample holder
5) oven.

Each of these parts is discussed in turn.

(1) Source of the applied electric field.

The 85 cps electric field is produced by an oscillator, amplified, and is coupled to the sample by an impedance matching transformer. This system is capable of supplying up to 20 watts to the sample over a range of sample impedance from 10^3 to 10^7 ohms at less than one percent total harmonic distortion.

Every effort is made to prevent the entry of any 60 cps into this system in order to remove the possibility of mixing of 60 and 85 cps signals which would produce a 25 cps component in the output. The oscillator and amplifier are operated with battery plate and filament supplies and are carefully shielded and mechanically isolated from the laboratory floor. The whole system is placed in a region of minimum magnetic field. The net result is that at all

levels of operation the amount of 25 cps produced by this system appearing across the sample is undetectable by the Hall voltage measurement system, even when the 60 cps electromagnet is operating at peak strength.

The 85 cps oscillator, shown in Figure 4, is of the Wien bridge type and is similar to the one used by Levy. Silver mica capacitors and one percent precision deposited-carbon resistors are used in the bridge circuit because of their stability and their low and opposite temperature coefficients. Precision mica or silver mica capacitors and precision wire-wound or deposited-carbon resistors are used whenever possible in all of the electronic equipment. The frequency drift of the oscillator is caused mainly by slowly shifting plate supply voltages from the battery supply but is less than ± 0.1 cps per 60 seconds. The oscillator frequency is checked before and after each measurement.

The output of the 85 cps oscillator is fed into the amplifier shown in Figure 5. The phase inverter is of the common-plate-load type of paraphase amplifier and allows an almost perfect ac balance of the push-pull output. The power amplification stage is a parallel push-pull arrangement using 5881 tubes. Harmonic distortion is reduced by the condensers across the primary and secondary of the output transformer. The variable winding-ratio impedance matching transformer has primary-to-secondary turns ratios of 0.144, 0.288, 0.576, and 1.000. The voltage and current supply to the sample are monitored by meters which are calibrated to ± 2 percent.

The leads carrying the 85 cps from the source to the sample are shielded and placed in regions of minimum magnetic field. The leads are arranged to enclose essentially zero area perpendicular to the magnetic field so that there is minimum pickup of 60 cps.

The battery plate supplies for the oscillator and amplifier are separate and eachuses a number of Burgess 21308 batteries connected in series. Heavily filtered conventional electronic power supplies are used for test purposes. Filament voltage is supplied from a pair of 6 v automobile batteries in parallel, which are continuously charged by a Mallory 12RS6DF power supply operating through external LC filters.

(2) Source of the applied magnetic field

The 60 cps electromagnet used is a modified version of the one designed and constructed by Levy. The modifications involved changing the configuration of the pole pieces and adding more turns of exciting coil. These changes gave a 20 percent higher usable flux density in the region of the sample.

The magnet coils and core are shown schematically in Figure 6. The exciting coils circle the upper and lower pole pieces and are connected in series. A parallel resonant circuit at 60 cps is formed by the magnet (~0.1h) and a capacitor bank (~70μf). The resonant circuit is driven from the 220 ac mains through a Variac and a 20:1 step-up transformer.

The current in the resonant circuit is monitored and, once the magnetic field is calibrated, is used to indicate the flux density of the magnetic field at the sample. The modified magnet yielded a maximum rms flux density in the region of the sample of about 1.2 weber/meter^2. The flux density B is related to the resonant current I by

$$B = 2.18 \times 10^{-2} \frac{(\text{weber/meter}^2)}{\text{ampere}} \; I \qquad (4.1)$$

in the linear region. The magnetic field is calibrated by using a search coil, which was about the same size as the samples, connected to a VTVM. The search coil was calibrated in a dc magnetic field by comparison with proton-resonance measurements. The flux density as indicated by the monitored resonant current is known to about ± 4 percent.

Cooling provisions for the magnet are twofold. The layer of exciting coil closest to the sample on each of the pole faces is made from hollow copper tubing through which cooling water passes. The pole pieces are protected from the heat of the oven by a layer of asbestos over which a flow of cool air is maintained.

The magnet is mounted on several layers of Isomode pads and sponge rubber so that almost no 60 cps vibrations reach the laboratory floor.

(3) Hall voltage measurement system.

The Hall voltage measurement system presented the most difficult design problems encountered in the experimental equipment. A system was needed with an input impedance in the tens of megohms, and inter-modulation distortion of 10^{-5} percent, and the ability to measure 25 cps Hall signals as low as 0.2 μv. The system described below meets these specifications.

The extreme linearity is required by the presence of large 60 and 85 cps signals in the Hall probe circuit. The signals result from the initial imbalance of the Hall probes, induced currents in the sample, and pickup voltages. The amplitude of these 60 and 85 cps signals may well be 10^6 times that of the expected Hall voltage. Thus, an ultralinear Hall voltage measurement system is required to prevent the mixing of these signals and the formation of spurious 25 cps signals comparable in amplitude to the Hall voltage.

The high sensitivity and the high input impedance are required by the low values of the expected Hall voltage and the high sample resistance.

Long-term gain stability of the measurement system is necessary since, in order to increase the detectability of the Hall signals, we want to use as long observation times as possible. The length of observation time is limited to about 60 seconds by instabilities in the amplitudes of the applied fields and variations in the oven temperature. However, it is desirable to make a complete run at any

given temperature before calibrating the Hall voltage measurement system. This requires a stable response over a period of about 15 to 30 minutes.

The band width of the measurement system should be as small as possible in order to increase the signal-to-noise ratio. A minimum band width of 1 cps was set by the instabilities in the frequencies of the applied fields and the response time for the system. The magnetic field frequency, over which we have no control, has a variation of about ± 0.1 cps per minute. The variations in the electric field frequency are of about the same magnitude. In order to allow a response time of about a second and to allow for unusual frequency drift conditions, the 1 cps band width was chosen.

The Hall voltage measurement system (Figure 7) consists of five parts: an input circuit, a preamplifier, an amplifier, a rectifier-integrator, and a recording device. The ac output of the system is monitored on an oscilloscope.

The input circuit (Figure 8) has to meet simultaneously the input impedance, linearity, and noise requirements and is the most critical part of the measurement system. It consists of three stages, each using a six-tube ultralinear cathode follower which was especially designed for this application[52]. The input stage has an effective input resistance of 10^{12} ohms and an input capacitance of about 10^{-11} f, thus giving an input impedance at 25 cps of about 10^{-9} ohms. However, the input impedance seen by the Hall probes is determined almost entirely by the wiring capacitance of the leads which connect the Hall probes

to the input circuit. The capacitance between the ungrounded Hall lead and the shield is minimized by driving this shield from the cathode of the input stage[53]. The driven shield surrounds the ungrounded Hall lead over its entire length except for that portion of the lead in the oven heating area. The grounded Hall lead is a thick copper tube which surrounds the driven shield. The total wiring capacitance for six feet of connecting cable is less than 10^{-10} f so that the input impedance seen by the Hall probes is about 10^{8} ohms.

The measured intermodulation distortion of the input stage is 2×10^{-5} percent or less up to signal input levels of 2 v. This was measured by inserting 60 and 85 cps on the input grid at 1:1 and measuring the amount of 25 cps produced. This high linearity is a consequence of the fact that the ultralinear cathode follower is in reality a plate-and-cathode follower in which both the plate and the cathode follow the grid voltage very closely[52].

The output impedance of the ultralinear cathode follower used here is about 0.5 ohm at 25 cps which provides an ideal source for the following filter network.

The noise level of the input stage, using a 1 cps band width and averaging the noise over 60 seconds, is 0.05 μv. The noise level of all three stages is 0.25 μv under the same conditions. Input signals smaller than these levels can be observed. In order to obtain this low noise the filaments of all of the tubes (in the measurement

system) were operated at 5.75 v, which gives an optimum signal-to-noise ratio for 12AX7's. Also, all components of the measurement system are carefully shielded and mounted on several layers of sponge rubber.

The second and third stages of the input circuit are band-reject filters of the Sallen and Key[54] type tuned at 85 and 60 cps. The all-over gain of the input circuit is less than 10^{-4} at 60 and 85 cps while being 1.3 at 25 cps. Frequencies above 50 cps are attenuated by a factor of at least 10^{2} by virtue of the RC low-pass filters inserted into the cathode feedback loops in series with the twin-T networks.

The preamplifier (Figure 9) consists of a series type amplifier stage[55,56] followed by a low-pass filter, 85 cps and 60 cps band-reject filters, and another low-pass filter, all filters being of the Sallen and Key type[54]. The amplifier stage has a gain of 100, contributes less than 0.05 μv of 25 cps noise to the system, and operates linearly within the range of signals at its input.

The amplifier (Figure 10) consists principally of three Sallen and Key[54] band-pass amplifiers tuned to give a band width at 25 cps of 1 cps. There is also a rejection filter for 35 cps, a frequency which appeared on and off throughout our measurements with an amplitude of 10^{-4} to 10^{-5} v. The source of this 35 cps signal is unknown, but it is produced by some effect proportional to the applied electric field and to the square of the magnetic field.

The all-over gain of the measurement system was 10^6 at 25 cps and 10^{-6} at 60 and 85 cps.

The rectifier-integrator uses a full-wave rectifier to convert the output of the amplifier to dc and then averages the dc signal over a variable length of time. The rectifying circuit was designed so as to be replaceable by a phase-sensitive rectifier which, however, we were not able to use in our measurements (see Chapter V). The time constant of the integrating circuit was variable from one to 60 seconds and the output level could also be varied. The gain of the total measurement system was sufficient to drive the recorder (Leeds and Northrup Speedomax Type G) to full scale (10 mv) with a 0.1 μv input.

The recorder, oscilloscope, and audio oscillator are operated from a doubly voltage-regulated power line to insure stable operation. The filaments and the plates of the measurement system are battery operated. Burgess N60 batteries are used for the plate supplies, and continuously charged (through elaborate filters) 6 v automobile batteries are used for the filament supply.

In the input of the measurement system there are provisions for reducing the level of the 60 to 85 cps picked up by the Hall probes to less than a volt so that these signals do not exceed the linear range of the input circuit. Two bucking sections (Figure 11) feed signals at 60 and 85 cps into the ground side of the Hall probe circuit. These signals are adjusted so as to be nearly equal in magnitude and

180° out of phase with the signals already present in the circuit. The 60 cps bucking section is supplied from a few turns of wire wrapped around the magnet core, and the 85 cps section is supplied from the primary of the output transformer of the primary electric field supply. Thus the signals produced by both bucking sections have exactly the proper frequency and automatically follow the variations in the field strengths. We were able to balance out the 60 and 85 cps picked up by the Hall probes to within a few millivolts, so that the adjustment of the bucking sections, once set, was not crucial. Either or both of the sections may be switched out of the circuit, and their relative positions in the circuit may be interchanged. The bucking sections were tested under normal operating conditions and found to produce less than 0.1 μv of 25 cps.

The output of each stage in the Hall voltage measurement system could be monitored by an oscilloscope so that the condition of the signal could be checked at each stage. Since it was necessary at times to examine signals of less than 10^{-7} v, the oscilloscope was provided with the preamplifier shown in Figure 12, which raised the oscilloscope sensitivity from 10^{-3} v/inch to 10^{-7} v/inch. The oscilloscope preamplifier could be tuned at any of the three frequencies of interest and had a noise level (at a 1 cps band width) lower than 0.02 μv.

(4) Sample holder.

The sample holder supports the sample in the middle of the oven while maintaining no mechanical contact with the oven and keeps the sample in the region of uniform magnetic field. It also provides

electrodes, lead in wires, and a means of varying the pressure exerted on these electrodes. The sample holder may be removed from the oven and replaced exactly in its former location without disturbing the oven. The ungrounded Hall electrode may be moved within narrow limits along the side of the sample while the sample is in place, so that the relative placement of the Hall electrodes may be varied during the measurements.

The design of the movable portion of the sample holder is shown in Figure 13. The bottom layer is a three inch by ten inch quartz plate fused to a Vycor support plate. Fused to this bottom layer are three quartz plates which provide walls around the sample and the slides. One Hall and one electric field electrode are held in place by these walls. The other electrodes are located on the ends of the slides as shown. The slides extend outside of the oven and are held in place by small springs, the pressure on which can be varied externally. The end slide which holds the movable Hall electrode in place is slightly tapered so that it can be moved along the side of the sample. The top layer, another quartz plate fused to a Vycor support plate, overlays the sample, electrodes, etc., in order to keep them in place and to electrically insulate the leads from the oven wires.

The three layers which make up the movable portion of the sample holder are assembled with the sample electrodes and lead-in wires in place and then slid into the oven on a track. The orientation of the sample is controlled by the track and by the fixed

portion of the sample holder. This latter is merely a Vycor support plate which has a quartz stop fused onto its top. The movable portion slides along the Vycor plate until it comes to rest against the stop (Figure 14). Two views of the sample holder in place are given in Figure 15.

All of the quartz is 1.5 mm thick optical grade fused quartz obtained from Amersil.

The electrode configuration is shown in Figure 16. The lead-in wires (0.005 inch Pt wire) for the applied field electrodes are contained in a double bore ceramic tube which is surrounded by a grounded shield to the edge of the oven heating area. The lead-in wires are arranged so that they present essentially zero area to the magnetic field. The applied electric field electrodes are made of a double layer of 0.001 inch Pt foil and cover the entire end of the sample. The lead-in wire going over the top of the sample holder is insulated from the oven wires by a thin quartz plate which is not shown in Figure 16.

The Hall probe lead-in wires (0.005 inch Pt wire) lie in grooves in the top of the middle layer of quartz plates. The Hall electrodes are formed from the U-shaped portion of the end of the lead-in wires looped over the quartz plates. It was found that in order to maintain a low resistance contact with the sample about 0.5 mm of the wire should touch the sample. The movable Hall probe is the ungrounded electrode, and its lead-in wire is surrounded by a driven shield which extends to the edge of the oven heating area. The geometry of the Hall lead-in wires is shown in Figure 17. The grounded Hall probe

lead-in wire is led over the top of the magnet and is adjusted so that there is a minimum of 60 cps induced in the Hall probe circuit. In practice the 60 cps bucking section is rarely needed.

The lead-in wires, etc., are additionally shielded from external influences by the presence of a 20 gauge copper box which completely surrounds the magnet, oven, and sample holder.

The sample holder is supported by a non-metallic frame which rests on a layer of sponge rubber. It is completely isolated from the vibrations of the magnet. The position of the sample holder may be adjusted for optimum sample location.

(5) Oven.

Surrounding the sample in its holder on four sides is the oven, which is designed to maintain a uniform temperature in the region of the sample in the range from room temperature to 900°C. The oven is physically isolated from both the sample holder and the magnet by a 1/16 inch air gap and the oven is independently supported by a frame which rests on sponge rubber. The oven is open at each end to allow the insertion of the sample holder, but the smallness of the openings and the length of the oven insure a uniform temperature in the region of the sample.

The oven (Figure 18) is constructed from American Lava Corporation grade-A lava (hydrous aluminum silicate) which is a machinable ceramic material in its unfired form. The center portion

of the top and bottom of the oven is grooved with 56 slots in which the heating element is placed. The oven is held together with four lava bolts and nuts. The lava is machined to shape and then fired, forming a true ceramic.

The heating element is a 1/32 inch ribbon of Chromel A which is wound bifilarly in the grooves and is held in place with alundum cement. The heating element is supplied from a bank of ten 12 v automobile batteries connected in series. The batteries are continually charged from the 220 v dc mains through a series of filters except during an actual measurement. The slow discharge of these batteries and the consequent temperature variation during the course of a measurement limits the observation time for a Hall measurement to about 60 seconds. The large amount of ac hash which was always present in the dc mains prevented charging during a measurement, since the Hall electrodes are very sensitive to the presence of any ac signals in the oven circuit.

The thermal gradients present in the oven were checked by placing thermocouples at various locations in the oven. The temperature in the region of the sample was found to be constant to within a degree. This was also verified by the uniform melting of the surface of a NaCl sample held at its melting point for a short time.

The temperature of the sample was monitored by the sample conductivity rather than by thermocouples since the sample temperature was usually several degrees above the oven temperatures because

of ohmic heating. Moreover, it would be difficult to attach thermocouples to the sample without disturbing the electrical environment of the sample. We used the conductivity measurements of Etzel and Maurer[17] as our definition of the sample temperature in NaCl. These measurements were made on Harshaw NaCl and verified to within one percent by Levy[2]. Etzel and Maurer found the conductivity to be

$$\sigma = \frac{3.72 \times 10^{10}}{T} e^{-\frac{21,600}{T}} \quad (\text{ohm-meter})^{-1}. \qquad (4.2)$$

For AgCl we used the conductivity data of Ebert and Teltow[29].

3. Experimental Procedures

The samples of sodium chloride and silver chloride used in our Hall measurements were received in the form of single crystals cleaved (or in the case of AgCl, sawn) out of synthetic optical grade crystals grown by the Harshaw Chemical Company. The sample size was approximately 2.60 x 2.60 x 0.26 cm for both NaCl and AgCl.

Since the NaCl crystals were cleaved to the required size, the relative orientation of the crystal axes and the sample faces was known. With AgCl this orientation was unknown at the beginning of the measurements. However, the formation of dendritic growths of silver on and near the surface of the AgCl samples (see Chapter V) permitted a rough determination of this orientation.

The NaCl crystals were used as received from Harshaw, with no grinding or polishing, so that the samples would be as pure as possible. However, before attempting any Hall measurements, the

samples were annealed by raising their temperature at 5°/minute up to 760-780°C, holding this temperature for an hour, and then lowering the sample temperature at the same rate.

The AgCl crystals were received as sawn, except that the large top and bottom faces of the samples had been polished (by Harshaw) until fairly smooth and parallel. We then polished (with sodium thiosulfate) the ends of the sample over which the applied electric field electrodes were to fit, so that the electrodes would make good contact with the whole end area. The AgCl samples received the same annealing as the NaCl except that the maximum temperature used was 420°C. The preparation of the NaCl samples involved no precautions against light reaching the sample, but attempts were made to shield the AgCl samples from violet and ultraviolet light. Both the NaCl and AgCl samples were shielded from light during the Hall measurements.

The Hall effect measurements were undertaken as follows. The samples were prepared, placed in the sample holder, and inserted into the oven. The temperature was raised at about 5°/minute up to the lowest temperature at which we might hope to observe a Hall voltage. Measurements were attempted at intervals of 20-30° as the temperature was raised toward the melting point. Measurements were also attempted on the downward portion of the temperature cycle.

At any temperature the measurement procedure involved recording: (1) the detection system noise (input shorted), (2) thermal noise of the sample (no applied fields), (3) noise associated with the

magnetic field, (4) noise associated with the electric field, and (5) the noise-plus-signal (if any) with both applied fields present. Several values of the applied fields were used to test the proportionality of any observed signal to the magnitude of the applied fields.

The observed thermal noise corresponded to the measured sample resistance unless the Hall electrodes were not making a good contact with the sample. The application of the magnetic field did not cause a measurable increase in the observed noise level above thermal noise. However, a large amount of noise was always associated with the application of the electric field (see Chapter V). The presence of a Hall signal would manifest itself as an increase in the average signal level with both fields present over the average signal level with only the applied electric field present.

The magnitude of the recorded signal levels is calibrated by using an artificial source of 25 cps, whose magnitude is known. After each series of measurements the artificial 25 cps source is switched into the input of the measurement system. The output of the artificial source is adjusted until the recorder indicates the levels recorded during the measurement.

The sign of the observed Hall signal can be determined by comparing its phase with the phase of a reference signal. This comparison is made by observing the Lissajous figure produced by the Hall and reference signals on an oscilloscope. The reference signal is calibrated by making a Hall measurement on a germanium sample of of known majority carrier type[2].

The accuracy of the Hall voltage measurement depends on our ability to distinguish small differences in average signal levels. This in turn depends on the variability of the signal level in relation to the size of the difference in signal levels and on the accuracy of our artificial source. We estimate that we should be able to measure the difference in signal levels to ± 0.2 μv over the range of signals encountered if the noise level is fairly stable.

The precision of the measurement of the sample temperature depends upon our knowledge of the primary voltage, primary current, and sample dimensions. The sample size is measured with a micrometer to within 0.1 percent, and the voltage and current are known to within two percent. The fractional error $\Delta\sigma/\sigma$ associated with the conductivity is 2.8 percent, which gives a fractional error $\Delta T/T$ for the temperature of 0.2 percent for NaCl and 0.3 percent for AgCl[2].

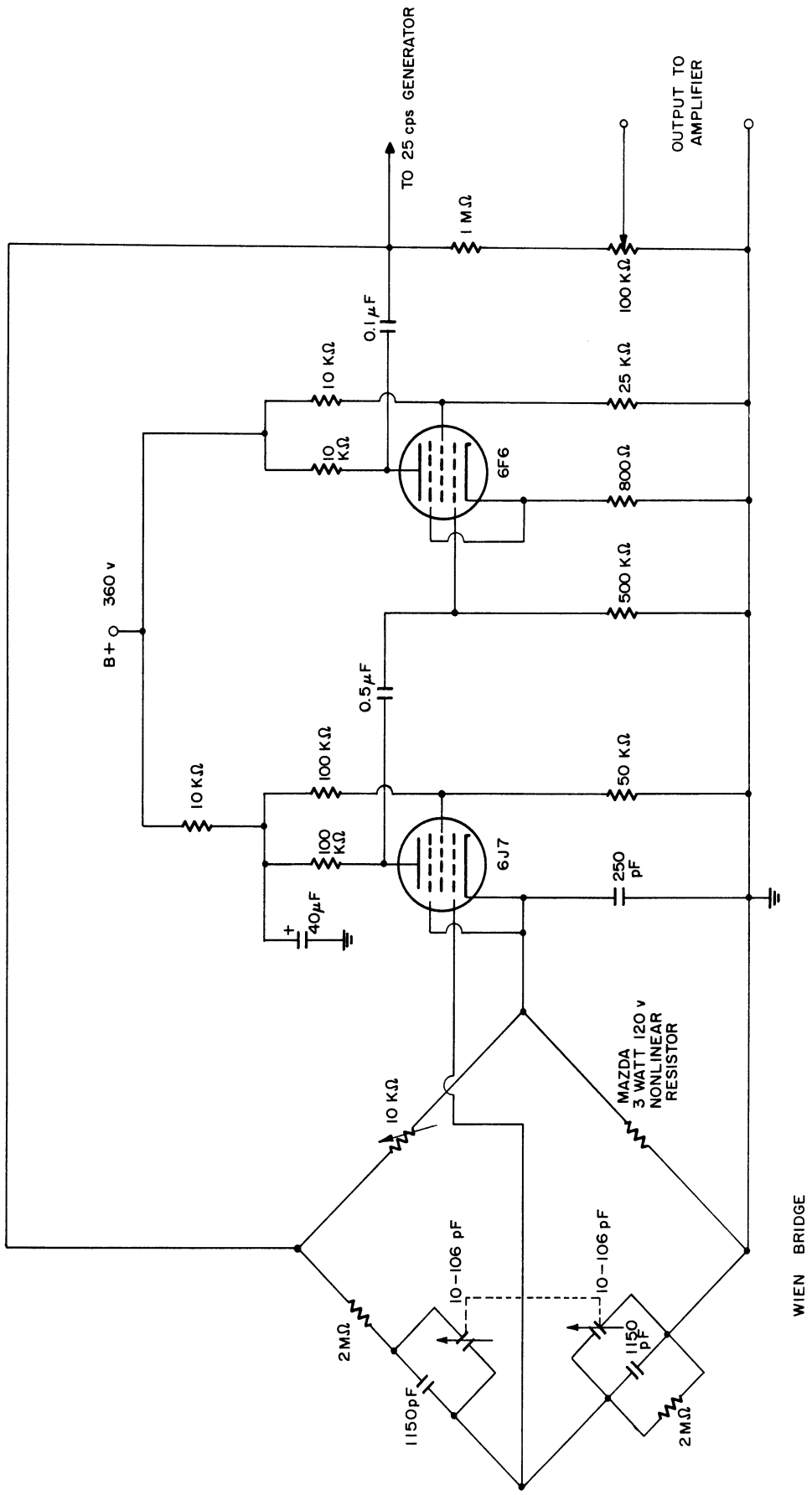

Figure 4. 85 cps Oscillator.

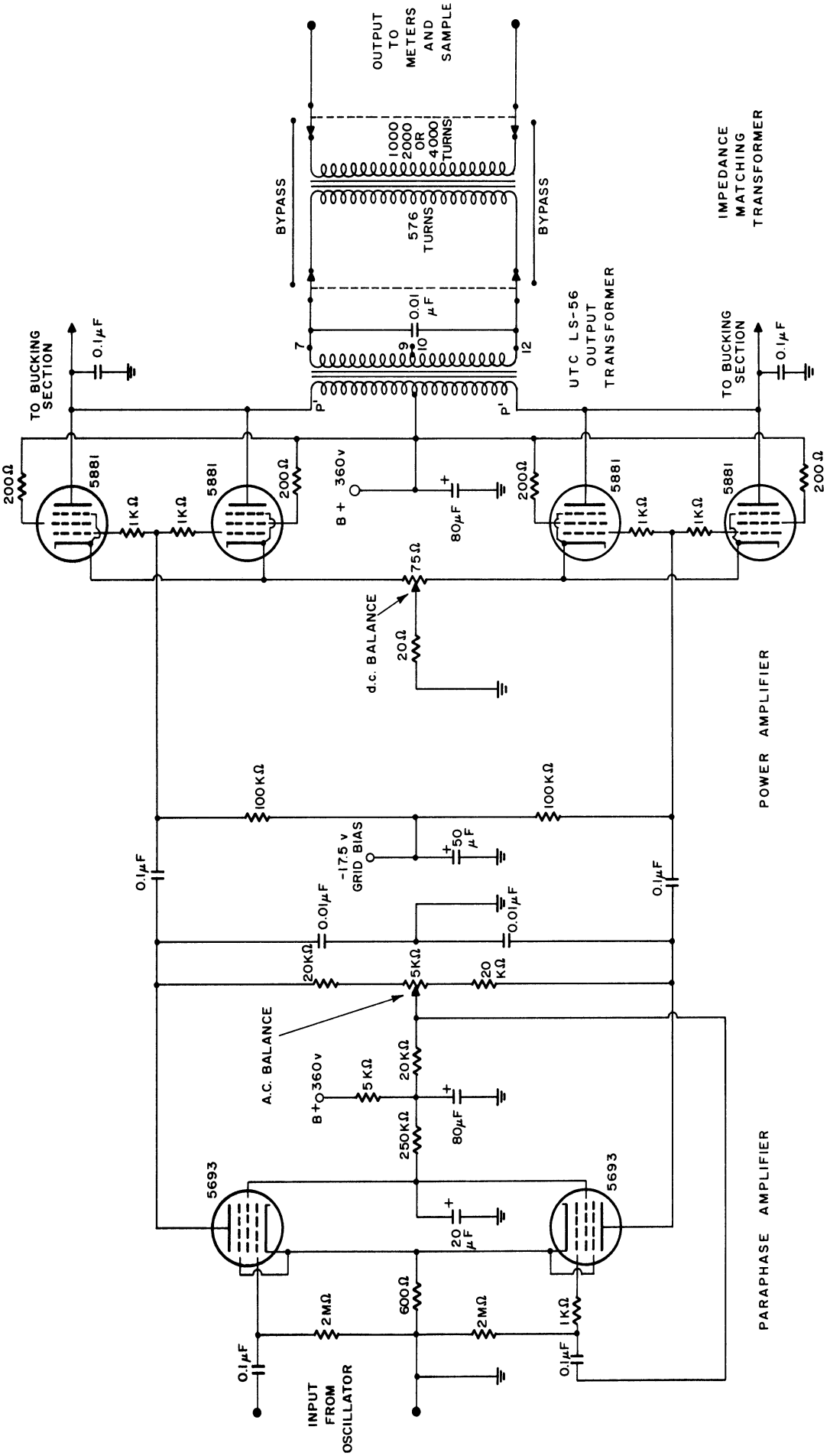

Figure 5. 85 cps Amplifier.

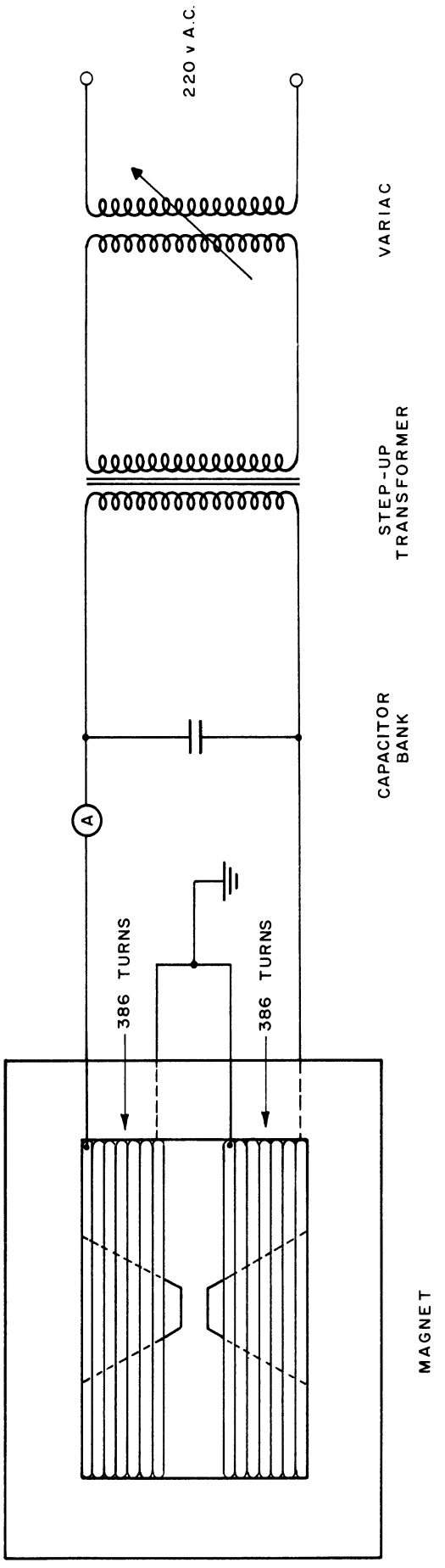

Figure 6. Magnet Power Supply.

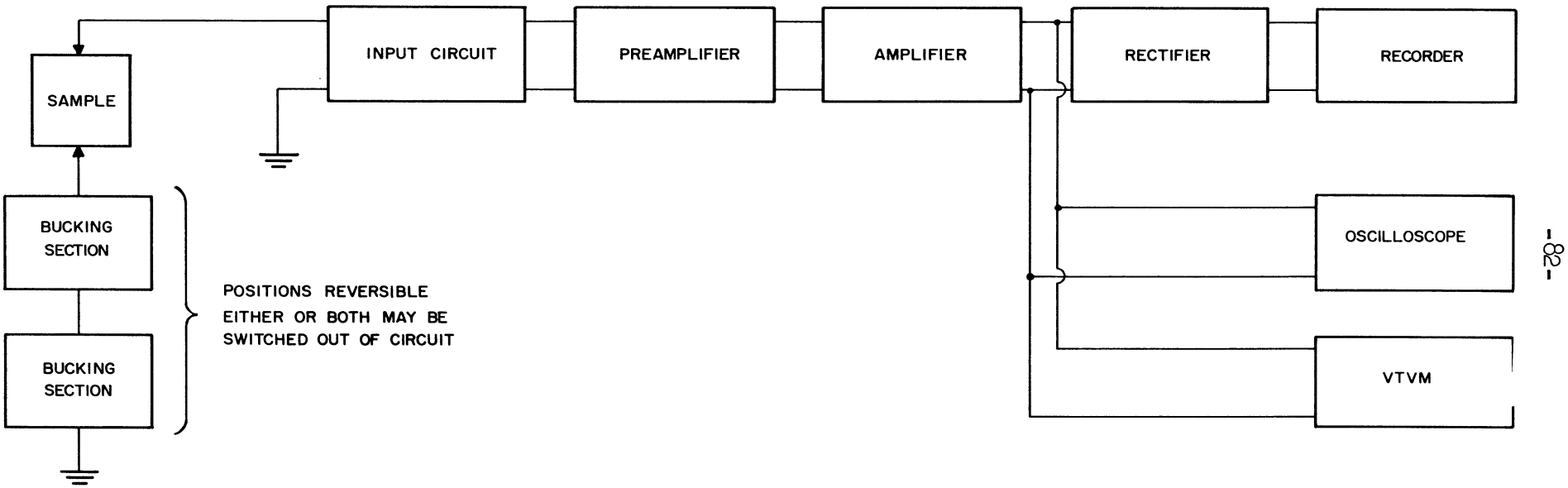

Figure 7. Hall Voltage Measurement System.

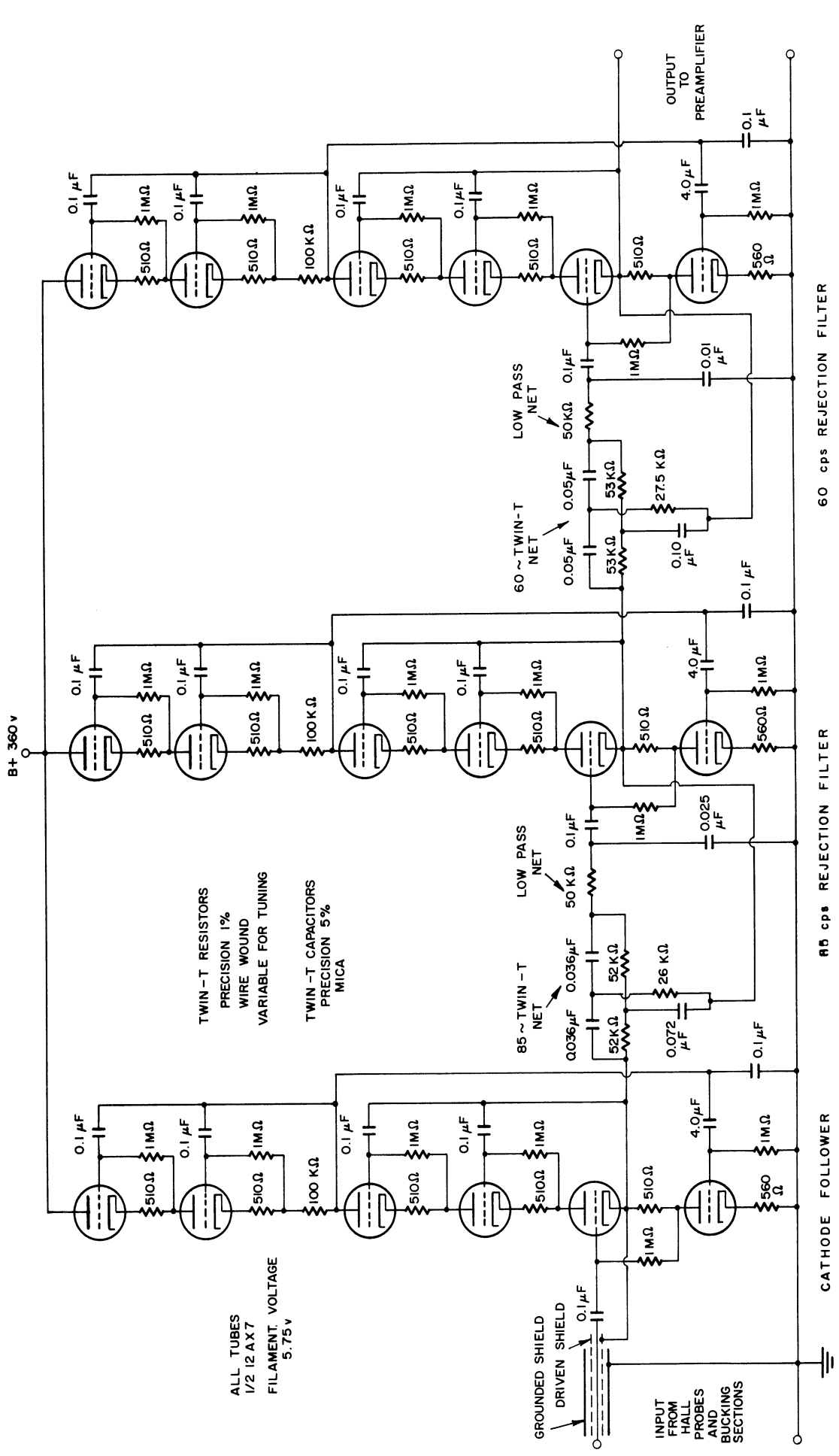

Figure 8. Input Circuit.

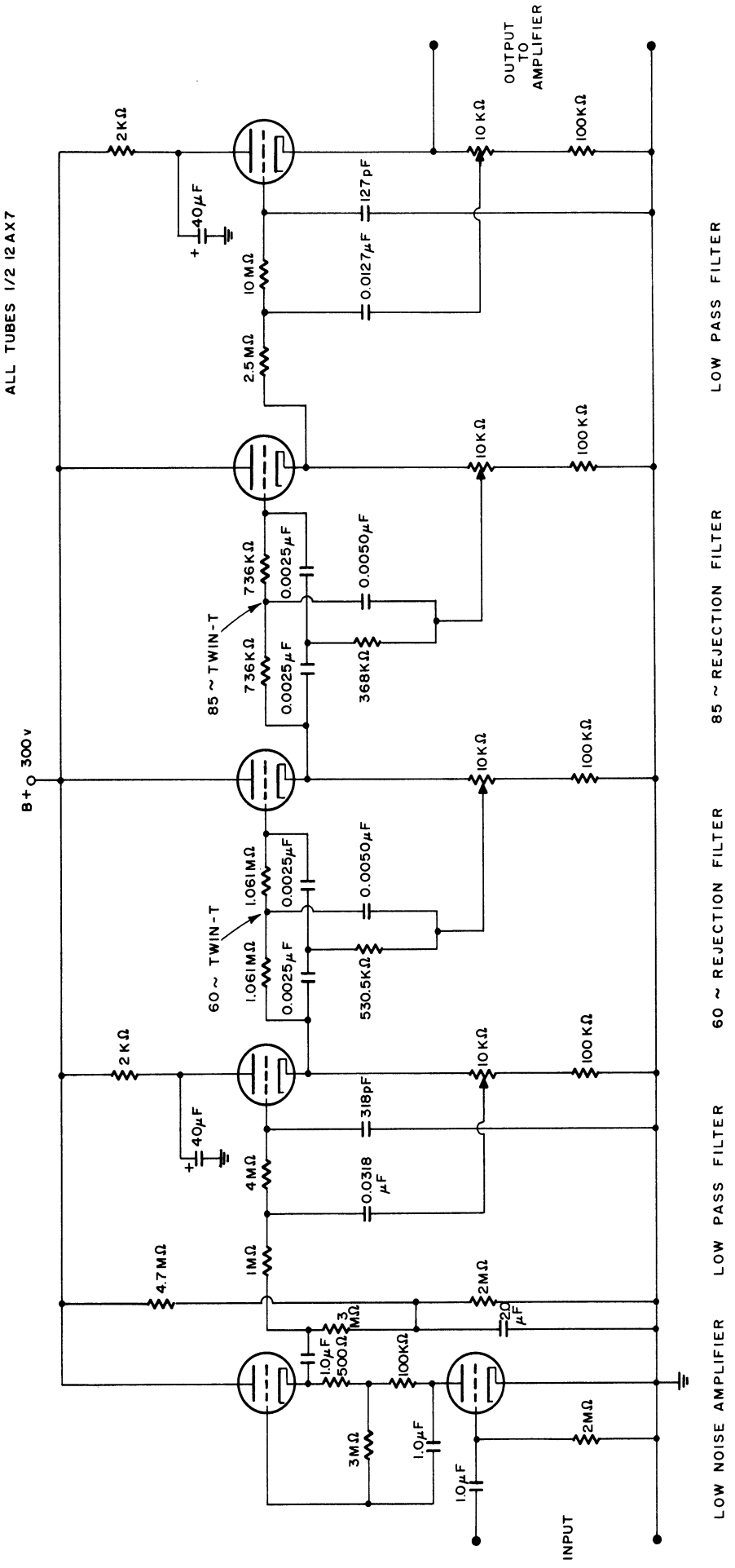

Figure). Preamplifier.

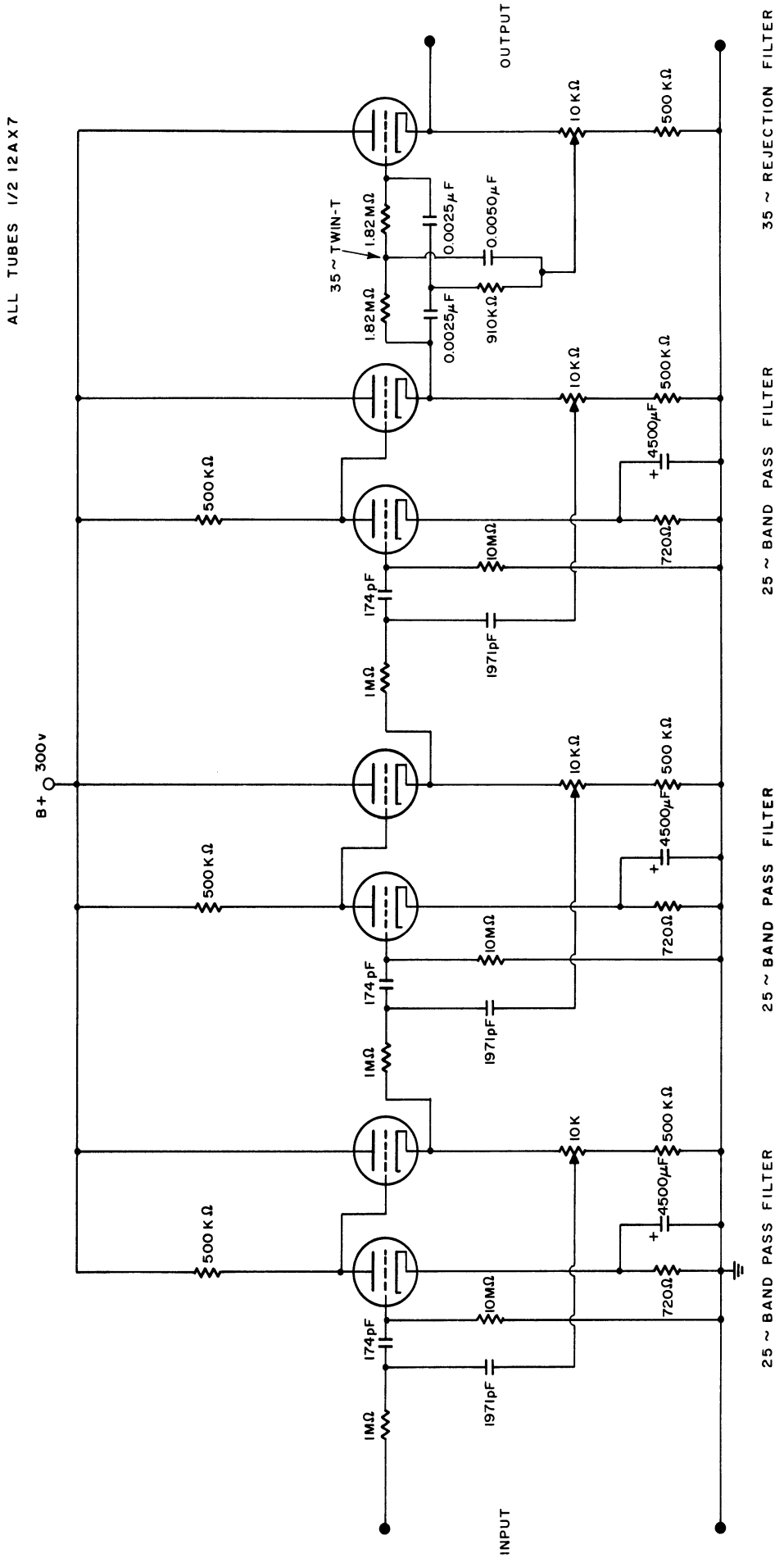

Figure 10. Amplifier.

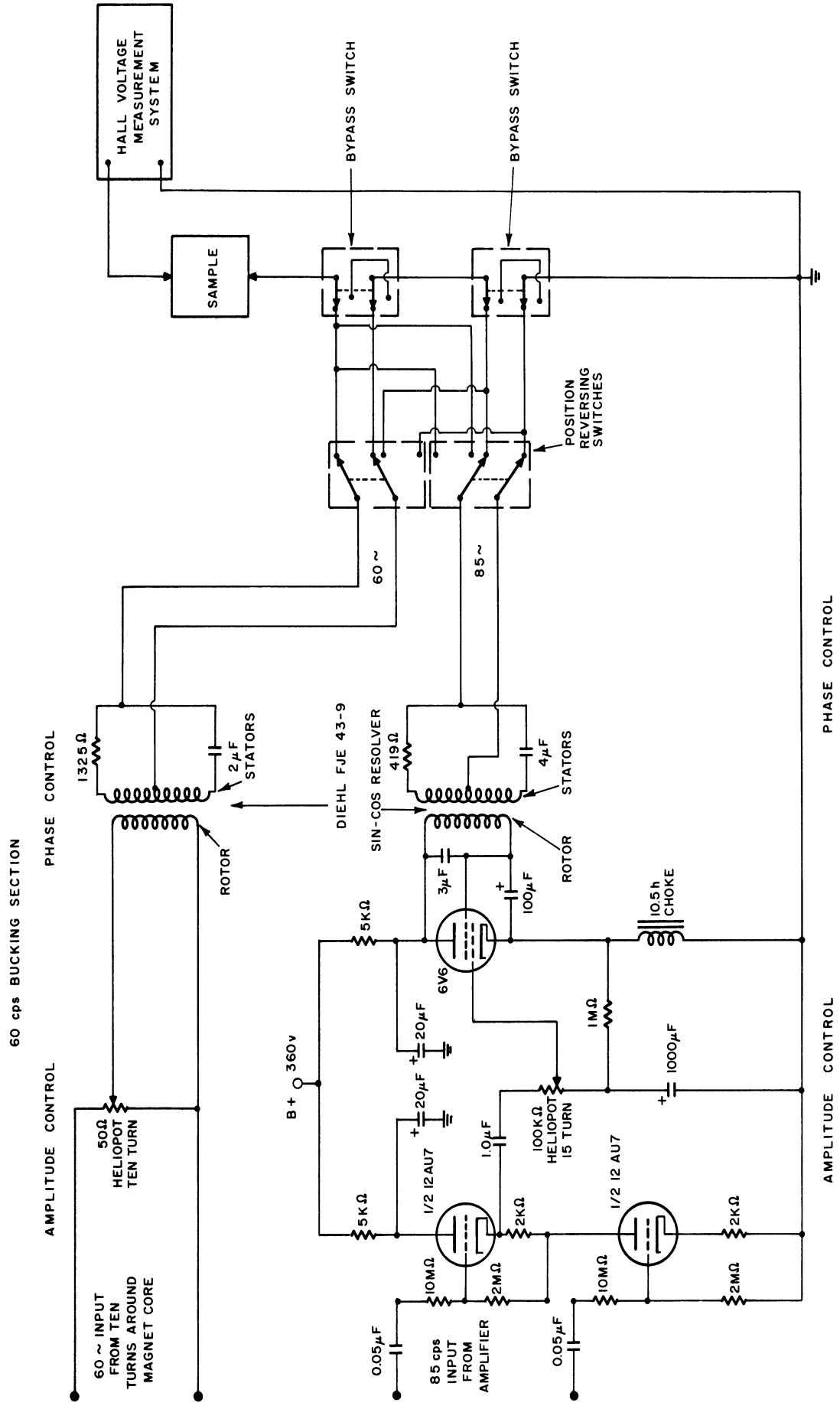

Figure 11. Bucking Sections.

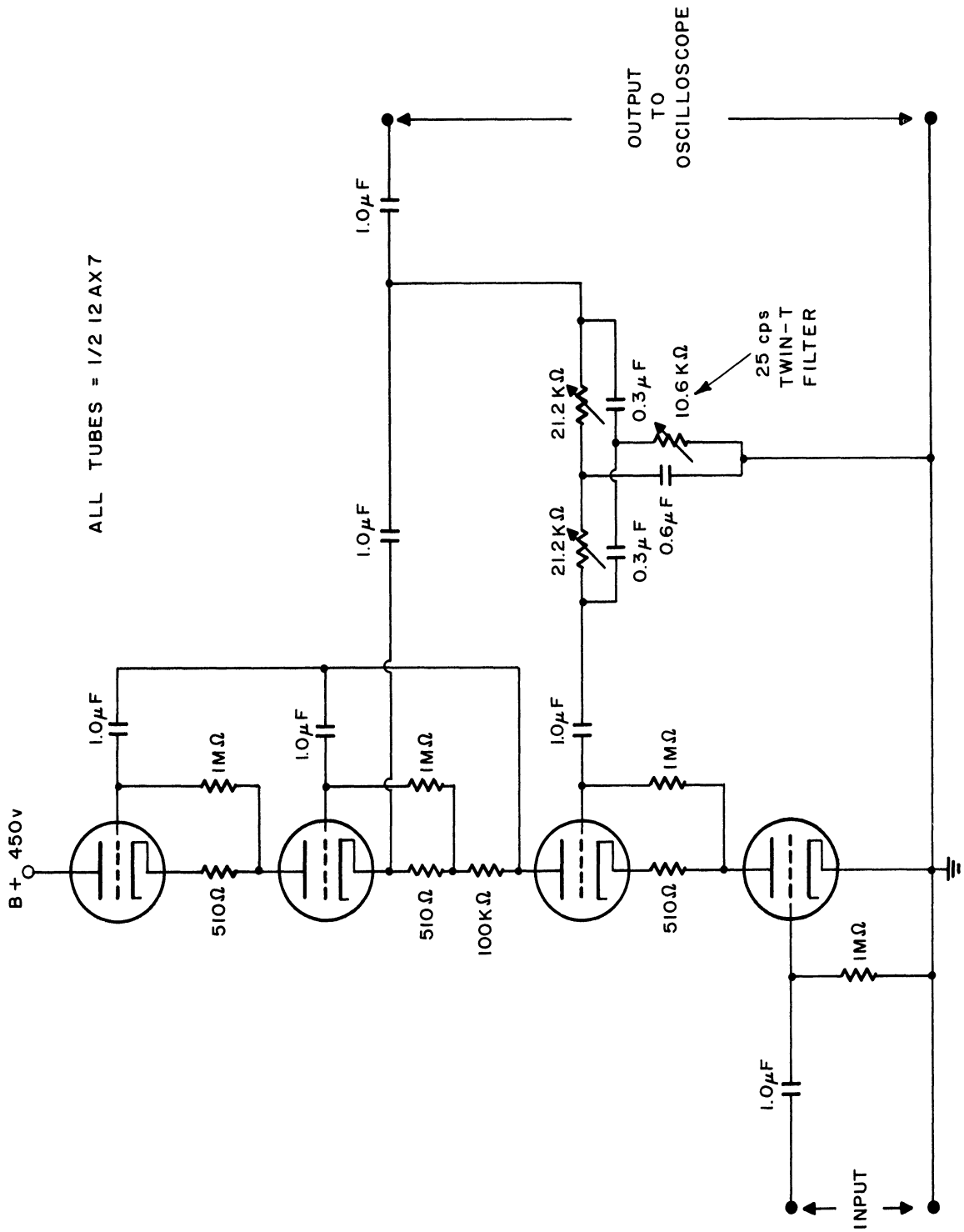

Figure 12. Oscilloscope Preamplifier

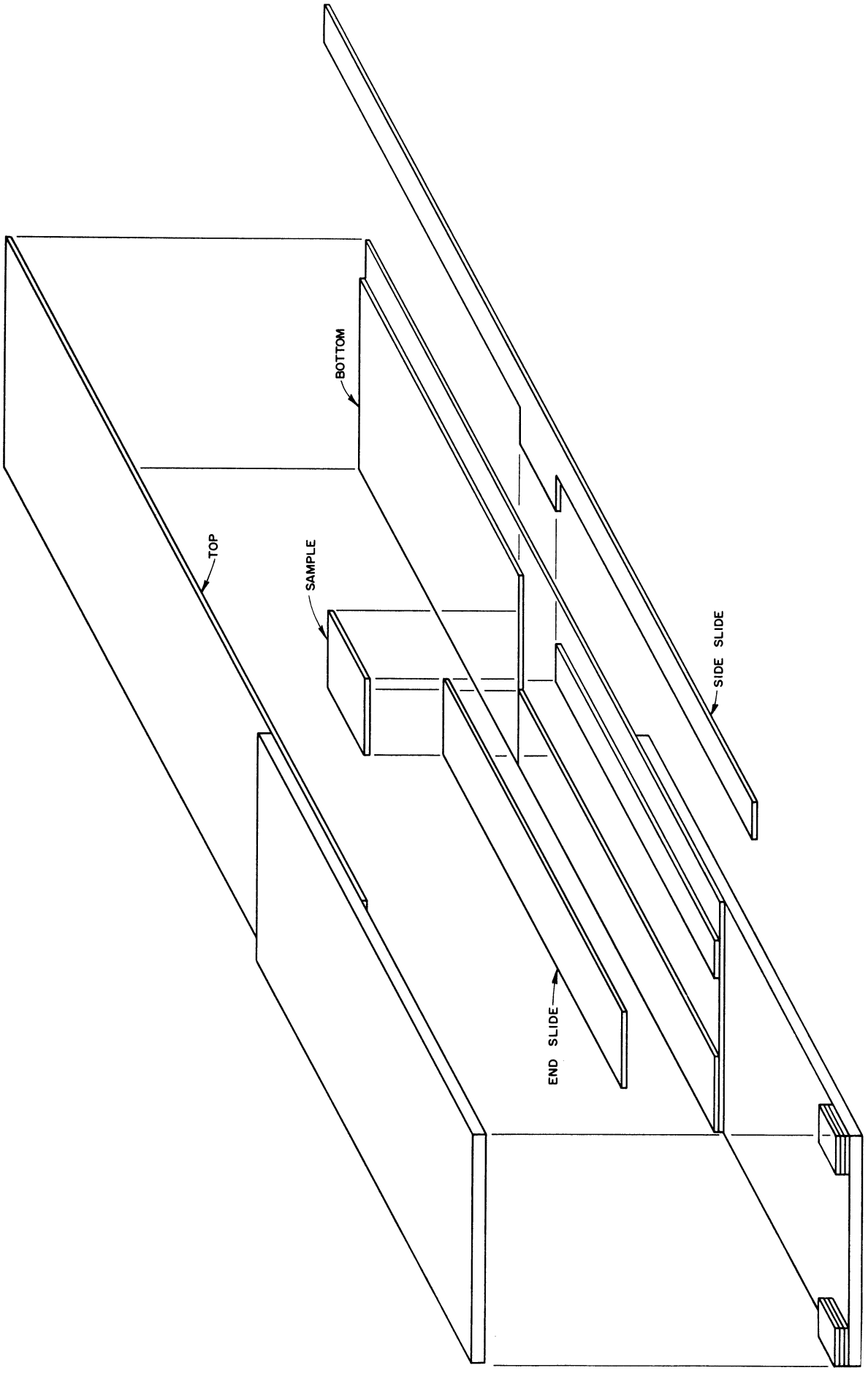

Figure 13. Sample Holder - Movable Portion

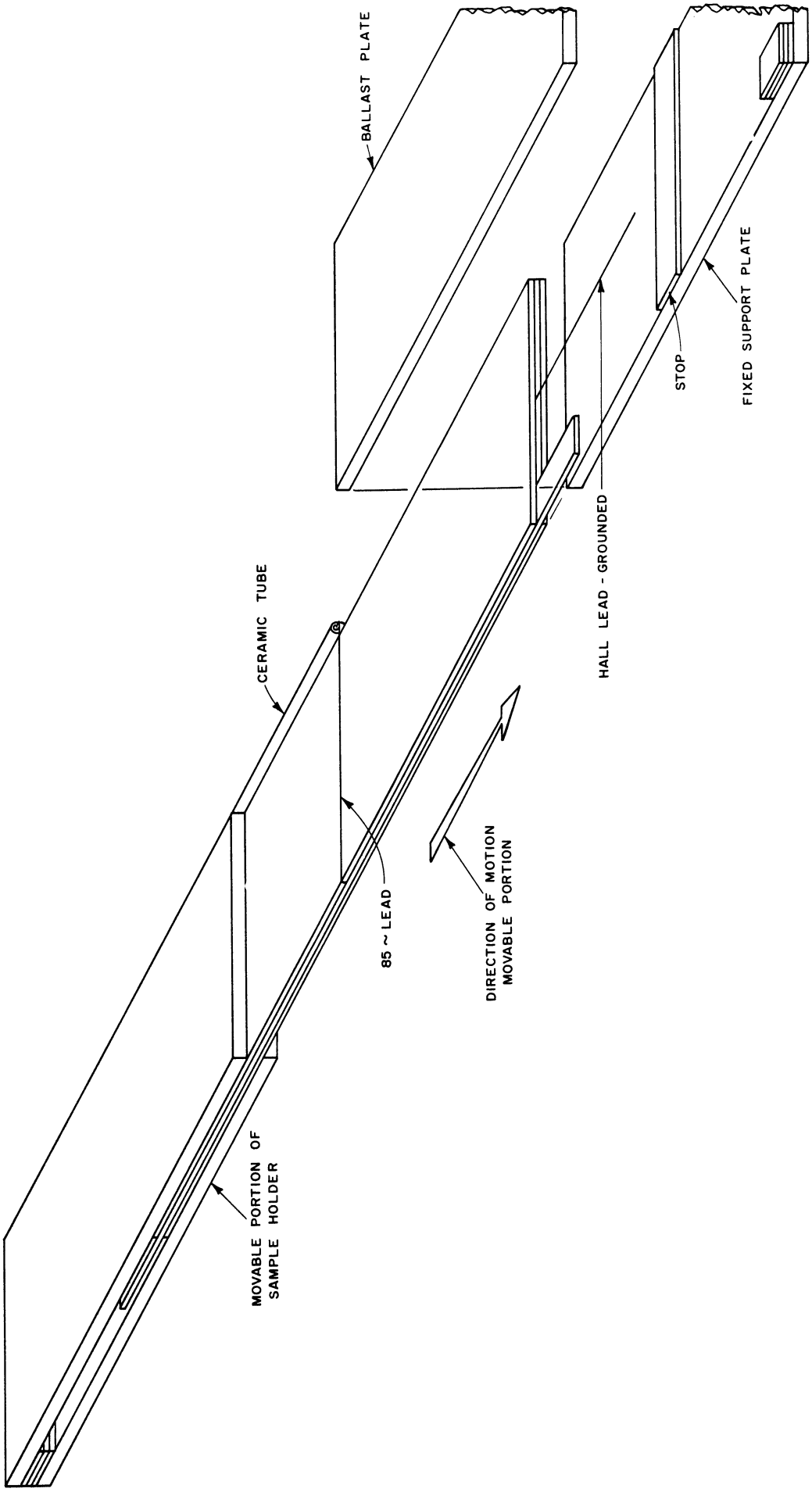

Figure 14. Sample Holder - Assembly.

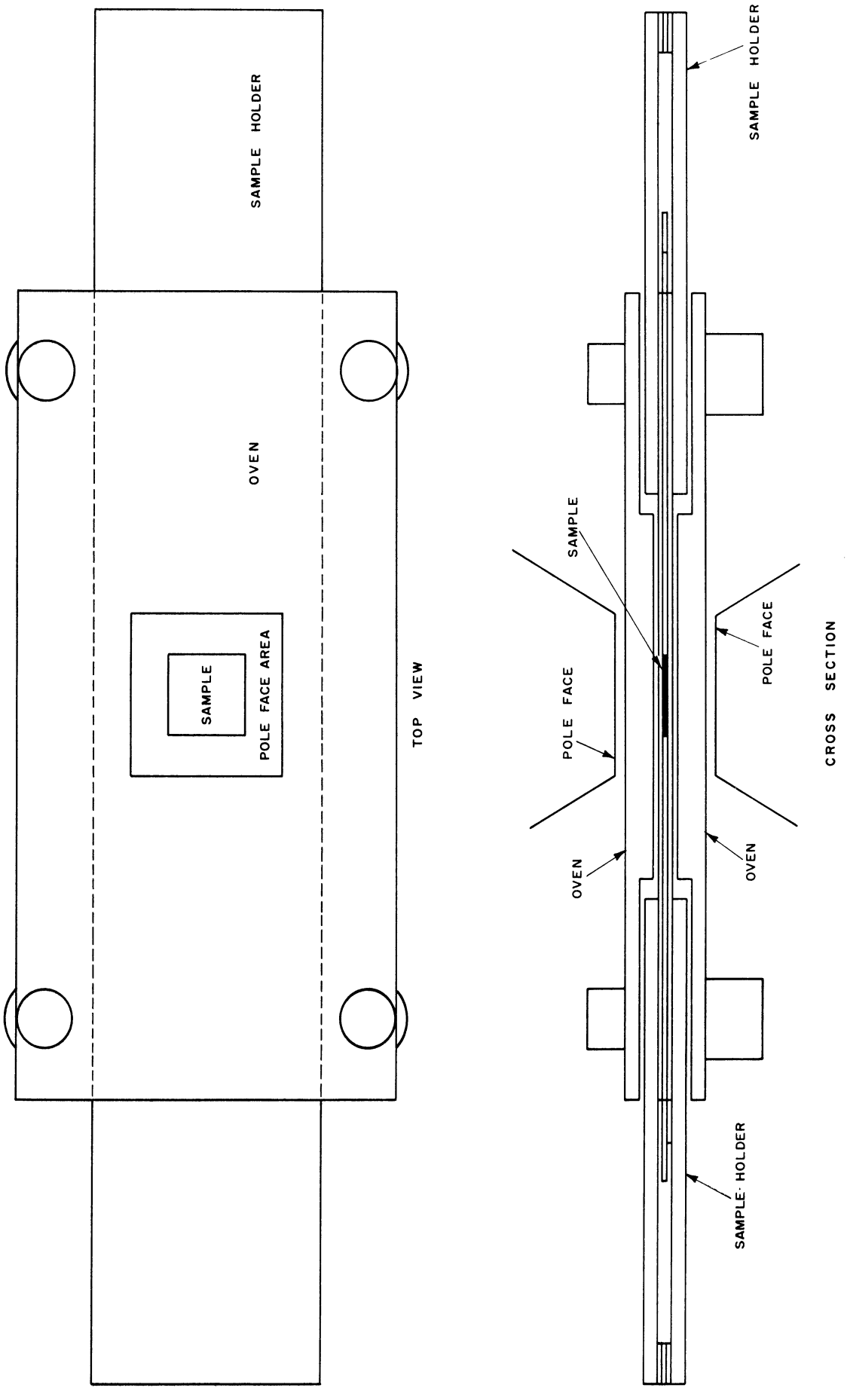

Figure 15. Relative Positions of Sample Holder, Oven, and Pole Faces.

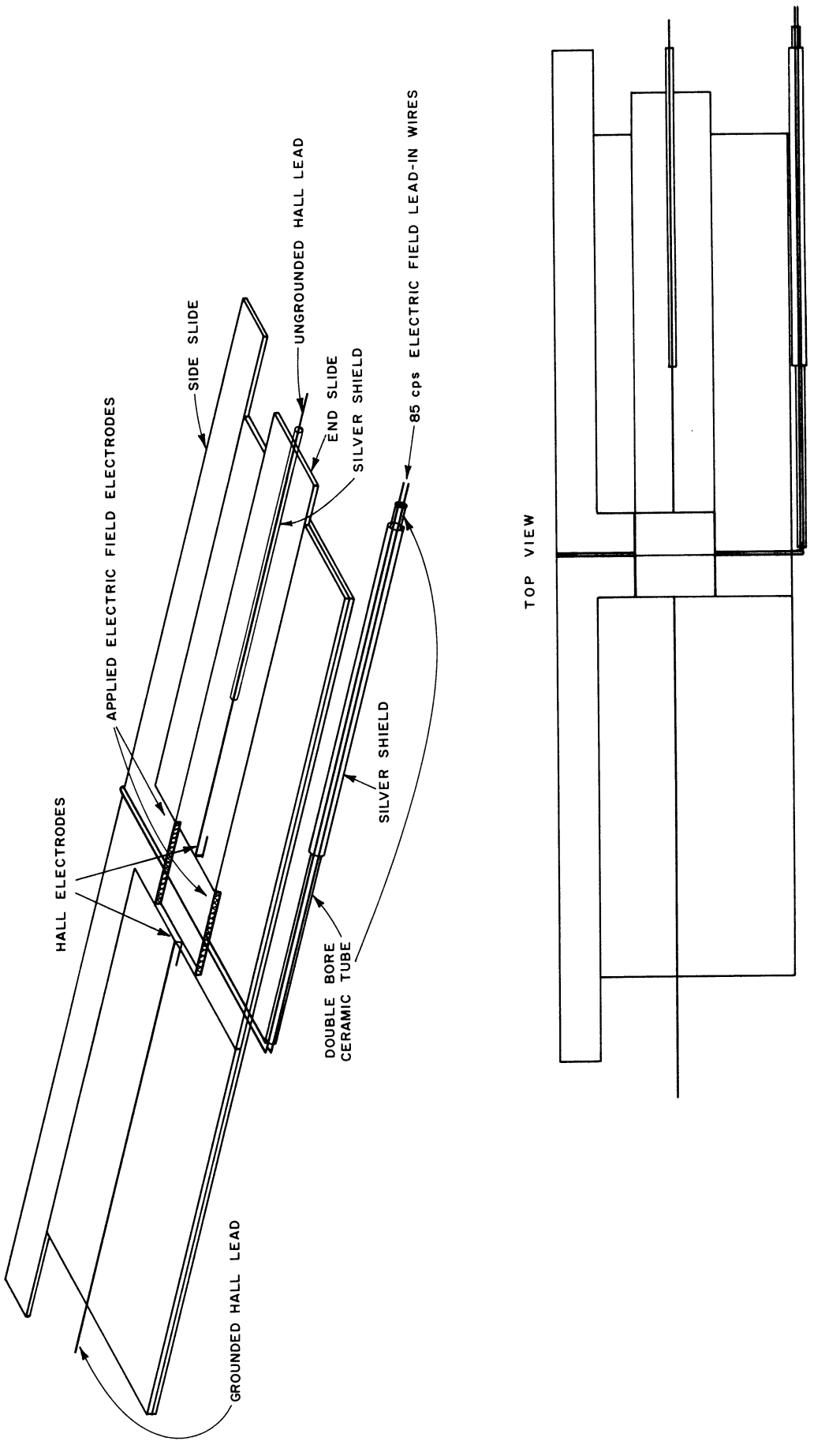

Figure 16. Electrode Configuration.

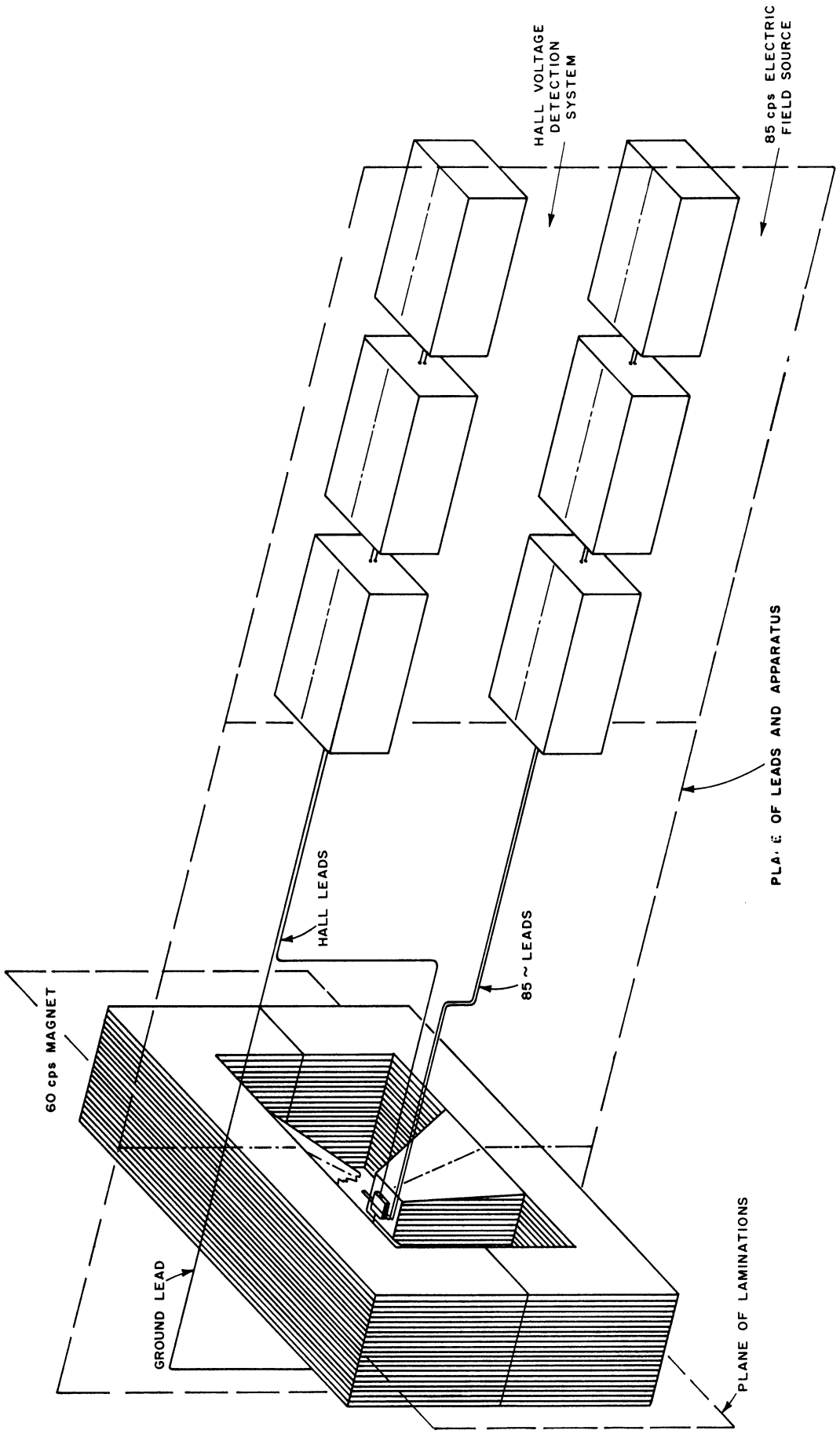

Figure 17. Location of Leads and Electronics with Respect to Magnet.

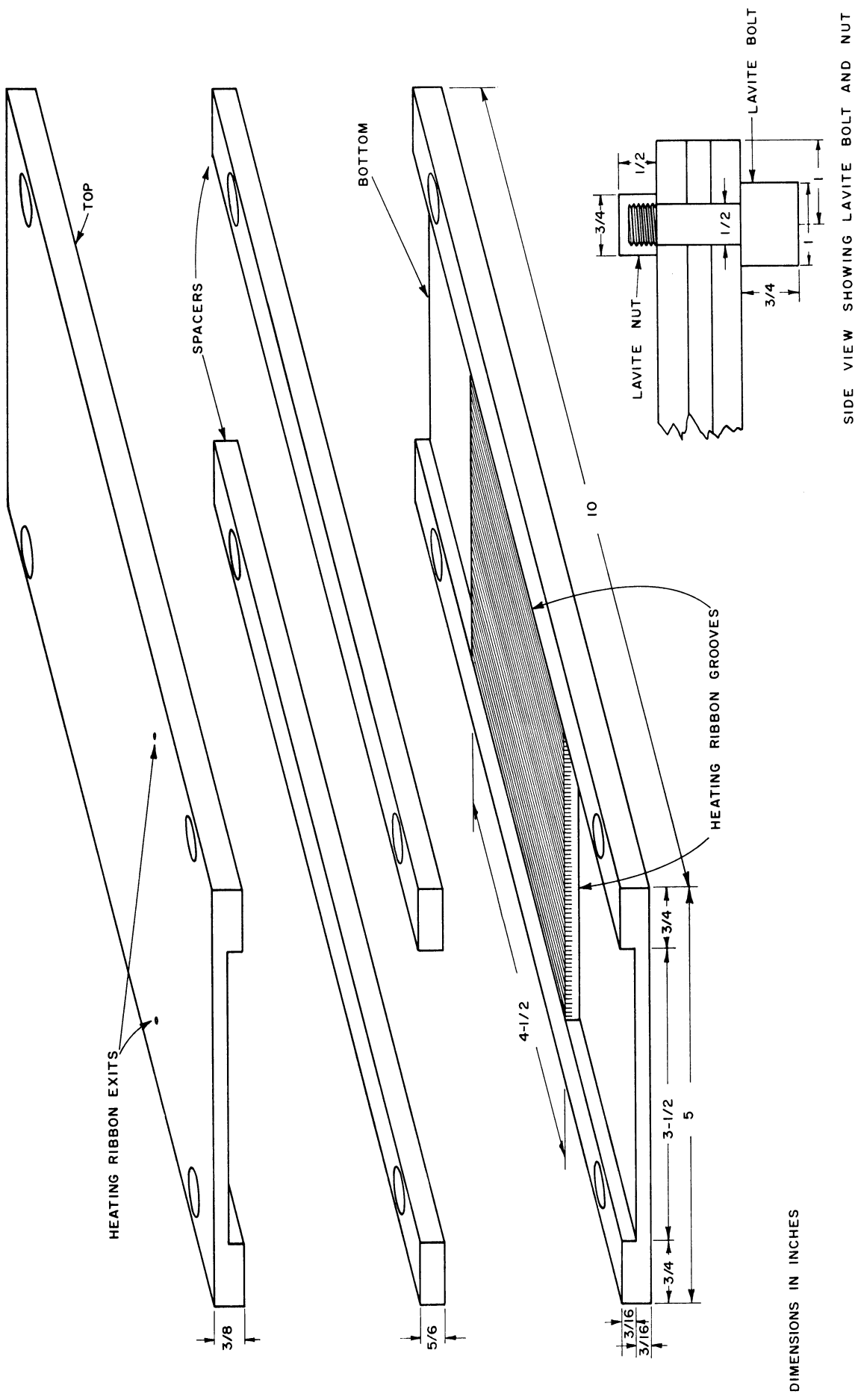

Figure 18. Oven.

CHAPTER V

RESULTS AND DISCUSSION

1. Hall Effect Measurements in NaCl

After our apparatus and procedures had been developed in their final form, we made several series of measurements of the Hall effect in NaCl. Each series followed a temperature cycle from room temperature up to within 10-50°C of the melting point (800°C) and back down again. In spite of the rather high level of current noise, we were able to make measurements of the Hall effect under fairly stable conditions at seven temperatures. We are fairly certain that the effect measured was in fact the Hall effect although there exists a slight possibility that some or all of the measured voltage was due to a nonlinear process at the sample-electrode interfaces. We shall examine these reservations in detail below.

Thus both the primary and secondary goals of our investigation were satisfied. That is, the Hall effect due to the motion of the ionic charge carriers in a pure ionic conductor was measured using the equipment which had been designed for this purpose. This represents the first Hall effect measurement in a pure ionic conductor.

The main obstacle encountered in making Hall measurements in NaCl was the presence of a large amount of noise with components near 25 cps. This noise was always associated with the passage of current through the sample; hence, we shall term it "current noise."

The current noise took two forms. First there was a component which appeared at all temperatures and whose amplitude was roughly proportional to the 85 cps current at low current levels. At higher currents the noise amplitude was proportional to a higher power of the current. This noise appeared continuously at all times that the 85 cps electric field was present. This "continuous" noise had a fairly uniform spectrum in the low audio frequency range. No temperature or pressure dependence of the continuous noise was observed. This is apparently the same noise which Levy[2] observed.

The second type of current noise occurred at irregular intervals and seemed to be uncorrelated with the continuous noise. It manifested itself as large amplitude bursts which lasted for a fraction of a second. These bursts ranged in magnitude from 5 to 50 times the level of the continuous noise at a given temperature. The burst noise exhibited a marked temperature dependence. As the temperature was raised the average interval between bursts became shorter and the amplitude of the bursts became larger. The size of the bursts was roughly proportional to the current although this was hard to measure. Under normal circumstances the burst noise occurred only when the 85 cps voltage was applied across the sample. However, single bursts could be induced by increasing the pressure on either the Hall or electric field probes, both with and without the applied electric field.

The continuous noise is probably caused by the same mechanism which produced the noise which obscured Levy's measurements. Levy did not remark about the occurrence of burst noise, but his visual averaging procedure would not be sensitive to a short noise burst.

The effect of the current noise on our observation of a Hall signal was twofold. First, the high level of continuous noise forced us to integrate the output of the Hall voltage measurement system over long time intervals in order to obtain significant data. Also, this noise was somewhat variable, even when averaged over this long period, so that it was not possible to set an absolute noise level at a given current and temperature. Secondly, the occurrence of the burst noise limited the length of the intervals over which we could average our output. This limited the accuracy of our measurements, especially at high temperatures where the bursts were closely spaced, since the nature of the Hall voltage measurement system allowed us to make measurements only in the quiet period between bursts.

In contrast to the noise associated with the application of the 85 cps electric field, no 25 cps noise was ever observed at the output of the Hall voltage measurement system when the 60 cps magnetic field was applied (with no electric field). The contribution of any noise associated with the magnetic field was at least a factor of ten lower than the thermal noise. This fact greatly simplified our measurement procedure.

It was not possible to eliminate the two types of current noise from our measurements. However, by designing equipment which was sufficiently stable to enable us to make a continuous Hall measurement over a period of a minute, and by recording the integrated output of the measurement system over this time interval, we were able to obtain usable Hall data at several temperatures in spite of the noise.

The measurement of the Hall effect is carried out by measuring the difference in the average amplitude of the 25 cps signal at the output of the measurement system before and after the application of the magnetic field (in addition to the electric field). Under the assumption that the noise associated with the magnetic field remains essentially zero in the presence of the applied electric field, the difference in the signal amplitudes represents a real effect. If we make the further assumption that the Hall effect is the only nonlinear process occurring within or at the boundaries of the sample, then we may attribute all of this difference to the Hall effect.

As noted in Chapter IV, the experimental equipment was carefully designed to preclude the possibility of any sources of 25 cps exterior to the sample. Thus, if a 25 cps signal is being generated, it is associated with processes occurring in the sample or possibly at the sample-electrode interfaces. It is difficult to conceive of a process occurring in the bulk of the sample (other than the Hall effect) which would produce the observed 25 cps signals. However, it is possible that a spurious 25 cps signal might be generated in a nonlinear contact between a primary electrode and the sample.

Arguments are presented below which show that the observed signal has the attributes of a Hall signal, and that the characteristics of the observed signal differ from those of a spurious signal produced by the nonlinear contact of a primary electrode and the sample. It seems likely that the nonlinear contact is not the source of the observed signals.

Thus, with the reservation that some or all of the observed difference in the average signal level upon application of the magnetic field may be due to an unknown nonlinear process at the sample-electrode interfaces, we may call the observed signal a Hall effect.

The observed Hall signal and the current noise on which it is superimposed are independent quantities so that the rms Hall voltage V_H may be calculated from

$$V_H = \sqrt{V_{S+N}^2 - V_N^2} \quad , \tag{5.1}$$

where V_N^2 is the mean square noise amplitude with only the electric field present and where V_{S+N}^2 is the mean square signal-plus-noise amplitude with both fields present. The Hall mobility corresponding to this Hall voltage is calculated by using Equation 3.28

$$\mu_H = \frac{2.10\ V_{H_{rms}}}{V_{rms}\ B_{rms}} \quad . \tag{5.2}$$

The Hall mobilities found at the seven temperatures are tabulated in Table III and are plotted in Figure 19. The experimental data from which these values are calculated are given in Table IV. The measurements of the observed signal difference were accurate to ± 0.2 μv, which corresponds to from 20 to 70 percent of the increase. The error flags shown in Figure 19 represent the range of mobility values corresponding to this measurement error. The uncertainties in the knowledge of the magnitude of the applied electric and magnetic fields are small compared to the uncertainty in the magnitude of the signal increase. The uncertainty in the temperature measurement is also indicated by error flags.

Our results are not accurate enough to permit the resolution of the apparent Hall mobility into the Hall mobilities of the sodium ion and chlorine ion vacancies. Our results, then, represent values corresponding to the difference in the sodium ion vacancy and chlorine ion vacancy mobilities in NaCl over the temperature range used. From the diffusion measurements of Laurent and Benard[44] and the transport number data of Tubandt et al.[23] given in Chapter II, we know the general shape of the curve which represents this difference in the carrier mobilities. Using Figure 2 as a guide, we have drawn a curve through our experimental data as shown in Figure 19.

From an extrapolation of the low temperature portion of a corresponding curve on a ln μT vs 1/T plot, we have calculated an activation energy and a pre-exponential coefficient for the mobility of the sodium ion vacancies in NaCl. These values are 0.87 ev and 2.0×10^{0} $(\text{meter})^2$-°K/volt-sec.

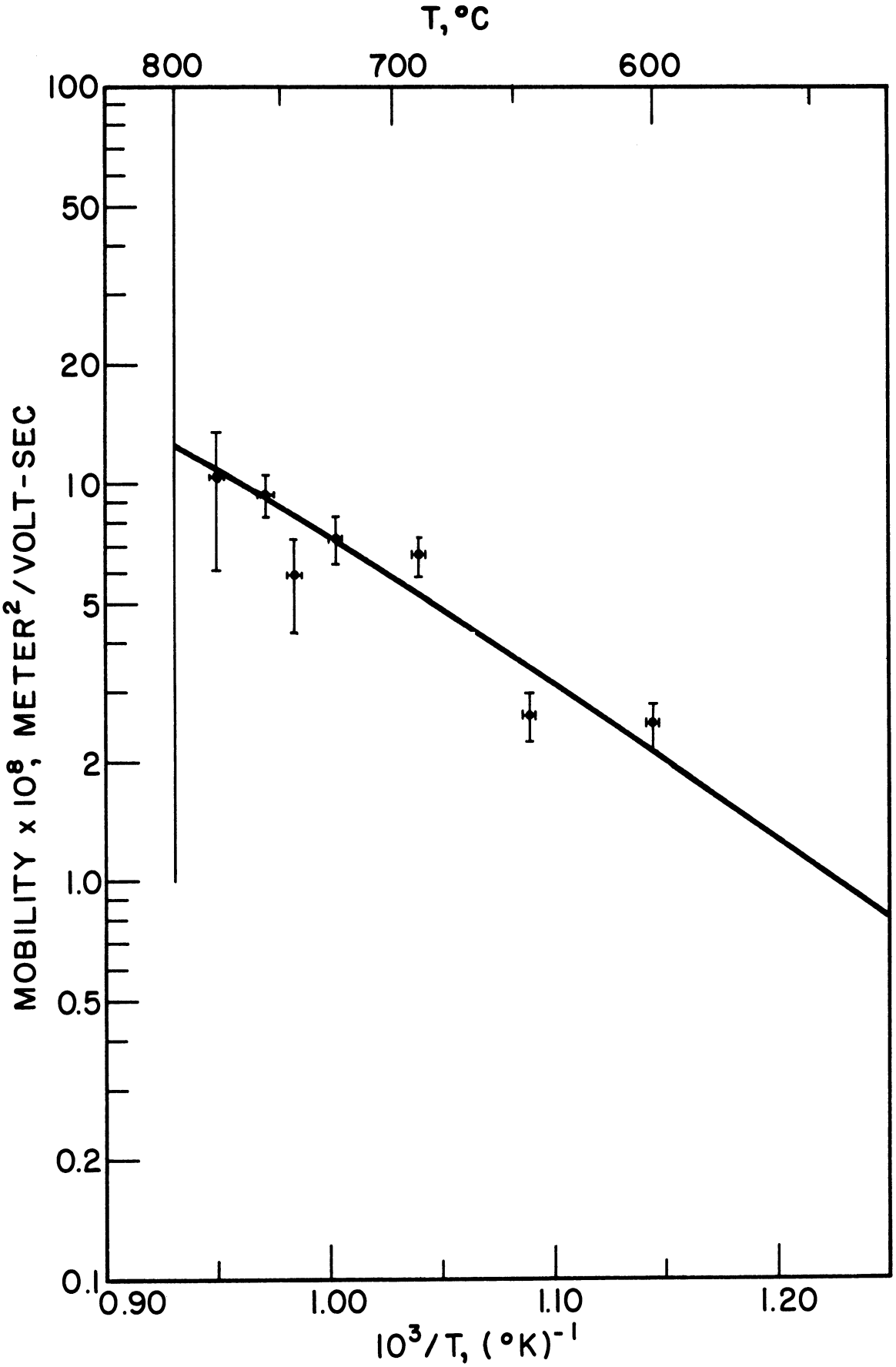

Figure 19. Hall Mobility Measurements in NaCl.

TABLE III

HALL MOBILITIES CORRESPONDING TO THE OBSERVED HALL VOLTAGE IN NaCl

Temperature (°C)	Hall Mobility x 10^8 ($meter^2$/volt-sec)
601	2.50
645	2.62
688	6.64
724	7.37
743	5.94
756	9.41
780	10.5

2. Discussion of Results

The results given above may either represent a true Hall effect in NaCl or they may be due to some other effect occurring within the bulk of the sample or at the sample-electrode interfaces. It is also possible that the two effects may coexist and that both may contribute to the observed increase in signal upon application of the magnetic field. In this case our results represent an upper limit on the Hall voltage and the corresponding Hall mobility in NaCl.

However, it is likely that the observed signals represent a true Hall effect, since the character of these signals is similar to that of a Hall voltage. First, the Hall voltage calculated from the observed signal increase is proportional to the magnitude of both the applied electric and magnetic field strengths. We were able to verify this proportionality for all but the 780°C reading. Fields used in the verification were lower than the fields used for the measurements quoted in Table IV. This resulted in a smaller signal increase and

TABLE IV

SUMMARY OF DATA - HALL VOLTAGE MEASUREMENTS IN NaCl

Run	Temperature Cycle	Applied Voltage v	Primary Current ma	Sample Resistance Kohm	Sample Temperature °C	Sample Temperature °K	1/T $(°K)^{-1}$	Flux Density weber/$meter^2$	Thermal Noise μv	Total Noise μv	Noise Plus Signal μv	Hall Voltage μv	Hall Mobility x 10^8 $meter^2$/volt-sec.
A	up	200	0.378	530	601	874	1.144	1.0	1.2	2.7	3.6	2.38	2.50
A	up	200	1.18	170	645	918	1.089	1.0	0.9	3.5	4.3	2.50	2.62
B	up	100	1.61	62	688	961	1.040	1.0	0.8	4.5	5.5	3.16	6.64
A	down	100	3.45	29	724	997	1.003	1.0	0.7	7.3	8.1	3.51	7.37
A	up	100	5.13	19.5	743	1016	0.984	1.0	0.7	9.8	10.2	2.83	5.94
B	down	100	6.67	15.0	756	1029	0.972	1.0	0.6	10.7	11.6	4.48	9.41
B	up	50	5.27	9.5	780	1053	0.950	1.0	0.7	10.2	10.5	2.49	10.5

thus, a larger uncertainty in the measurements. However, the proportionality was checked to an accuracy of about 20 percent as shown by the results tabulated in Table V. The Hall mobilities calculated from this low field data are shown in Figure 20, where for comparison the points given in Figure 19 are replotted. The calculated Hall mobilities from the high field and low field data were not averaged together because of the much larger uncertainties associated with the low field data.

We were not able to check the proportionality at 780°C because the high level of current noise prevented the detection of signals smaller than the quoted result. We were not able to use higher applied voltages across the sample since this increase was accompanied by a rapid increase in the amount of burst noise.

The second characteristic of the alleged Hall signal is that there was always an increase in the average signal level upon application of the magnetic field when such an increase was expected. That is, the signal was persistent and did not occur at some times and not at others.

The third characteristic of our Hall signal which would seem to indicate that it is a true Hall effect is that the Hall mobility which is calculated from the observed Hall voltages has the correct temperature dependence. It is unlikely that a spurious effect would have this same temperature dependence.

TABLE V

PROPORTIONALITY OF OBSERVED HALL VOLTAGE TO APPLIED FIELD STRENGTH IN NaCl

Temp. °C	Applied Voltage v	Flux Density $\frac{\text{weber}}{\text{meter}^2}$	Total Noise μv	Noise Plus Signal μv	Hall Voltage μv	Hall Mobility x 10^8 $\frac{\text{meter}^2}{\text{volt-sec}}$
601	200	1.0	2.7	3.6	2.38	2.50
	200	0.75	2.7	3.3	1.90	2.66
	100	1.0	1.7	2.0	1.05	2.21
645	200	1.0	3.5	4.3	2.50	2.62
	200	0.75	3.5	4.1	2.14	3.00
	100	1.0	2.1	2.5	1.36	2.86
688	100	1.0	4.5	5.5	3.16	6.64
	100	0.75	4.5	5.1	2.40	6.72
	50	1.0	2.6	2.9	1.28	5.38
724	100	1.0	7.3	8.1	3.51	7.37
	100	0.75	7.3	7.8	2.75	7.70
	50	1.0	4.1	4.3	1.30	5.46
743	100	1.0	9.8	10.2	2.83	5.94
	100	0.75	9.8	10.0	1.99	5.57
	50	1.0	6.1	6.3	1.57	6.59
756	100	1.0	10.7	11.6	4.48	9.41
	100	0.75	10.7	11.2	3.31	9.26
	50	1.0	6.1	6.4	1.94	8.15

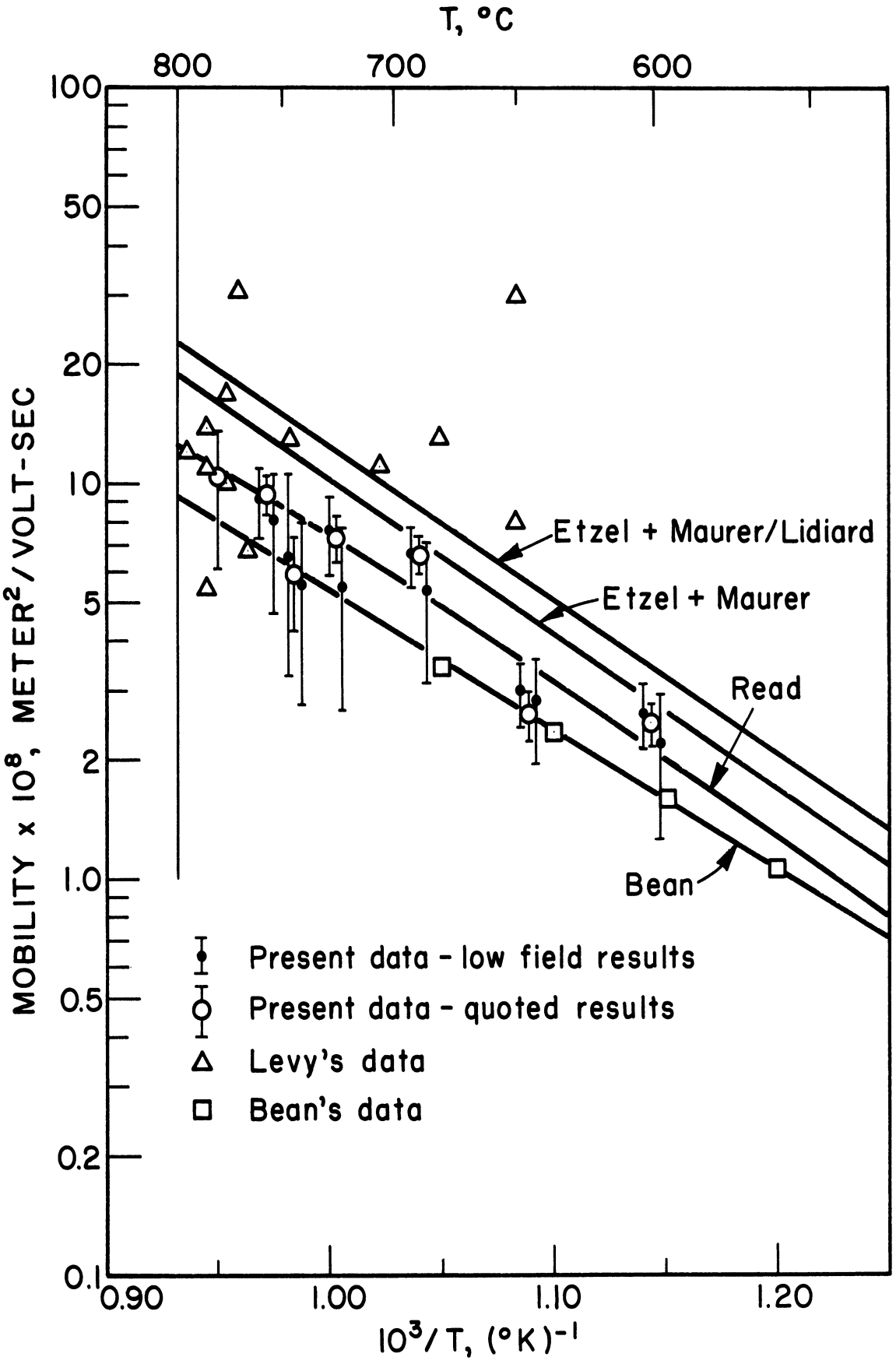

Figure 20. Comparison of Our Results with Previous Mobility Measurements in NaCl.

If a spurious signal were being generated at the sample-electrode interfaces, it would probably be sensitive to the electrode pressure. In general, the pressure exerted on the electrodes varied as the temperature was changed, and this pressure also varied from one series of measurements to another. The total variation in pressure was on the order of a factor of five. No pressure sensitivity of the signals was observed and the Hall voltages found in the various runs were fairly consistent. Thus, it would seem that contributions from spurious signals generated at the sample-electrode interfaces did not enter significantly into our measurements.

Next, the Hall mobilities calculated from our data are in the same range as those found by Bean[15] and by Etzel and Maurer[17] as is shown in Figure 20. Of course, our Hall mobility measurements represent the difference in the mobilities of the sodium ion and chlorine ion vacancies, whereas the Koch and Wagner type experiments of Bean and of Etzel and Maurer measured the mobility of the sodium ion vacancy. However, as noted in Chapter II, the mobility of the chlorine ion vacancy is low compared to the mobility of the sodium ion vacancy even at high temperatures. Thus the fact that our results are comparable to those found by Bean and by Etzel and Maurer is significant.

It can also be seen from Figure 20 that the curve which we have fitted to our data lies midway between Bean's curve and the curve representing an extrapolation of the data of Etzel and Maurer. Thus our results provide a rough check on the validity of both of these

former measurements although the uncertainty in our results does not allow us to choose which of these former measurements is the more accurate.

Our calculated value for the activation energy associated with the mobility of the sodium ion vacancies agrees fairly well with previous measurements given in Table I. Our value is higher than that found by Bean and by Etzel and Maurer but agrees exactly with the theoretical value of Guccione et al.[9]. This agreement is fortuitous since our calculated value depends on the slope of the curve fitted to our data at low temperatures where our data is sparse. Our value for the activation energy is accurate to about ±0.10 ev.

Although the pre-exponential coefficient associated with the mobility of the sodium ion vacancies found from our data is subject to even more doubt than our value for the activation energy, it is in rather good agreement with the coefficients found by Etzel and Maurer and by Bean listed in Table I. The extrapolation which we made gives a value which almost coincides with that found by Etzel and Maurer, but again this must be ascribed to chance. Values for the pre-exponential coefficient lying between 0.5 and 10 $(\text{meter})^2$-°K/volt-sec are possible, since the uncertainty in our Hall data allows some latitude in the extrapolation made.

The above comparisons are exact only if the Hall mobility of the ionic charge carriers in a pure ionic conductor is numerically equal to their drift mobility. However, as we pointed out in Chapter III, the Hall and drift mobilities differ at most by a factor which is of the order of magnitude of unity. Conversely, the approximate correspondence between our Hall mobility measurements and the previous drift mobility measurements supports this assertion.

It should also be noted that our results fall within the range of upper limits for the Hall effect in NaCl set by Levy[2]. This can be seen from Figure 20 in which Levy's results are plotted. If our results are interpreted not as a true Hall effect but as upper limits for the Hall mobility in sodium chloride, they set generally lower values for this limit than did Levy's measurements. Also, our measurements cover a somewhat wider range of temperature.

The fact that we were able to measure small differences in the average signal level and thus measure what seem deserving of being called a Hall voltage, whereas Levy was able to measure only the total noise amplitude, is due to: (1) our ability to record the output of the Hall voltage measurement system over relatively long time intervals, (2) our ability to average the amplitude of this output over these intervals, (3) the development of apparatus which was sufficiently stable to allow us to measure continuously over these long time intervals, and (4) the development of apparatus, especially the Hall voltage measurement system, in which we could be sure that no spurious 25 cps signals were being created.

We attempted to determine the phase of the alleged Hall signal and the relationship of its phase to the phase difference of the applied fields. The fact that the level of current noise was usually several times larger than the signal completely obscurred the signal phase so that it was not possible to monitor it. For this reason we did not use a phase-sensitive rectifier which had been designed for use with the integrating circuit. The phase of the V_{S+N} signal as observed in the oscilloscope at the output of the measurement system seemed to be only slightly less random than the observed phase of V_N, although such a visual phase check is admittedly crude. If we had been able to determine that the phase of the observed signal was equal to the phase difference of the applied fields, we would have had added reason for attributing the observed signal to a Hall effect.

Our inability to monitor the phase of the observed signal also meant that we could not determine the sign of the dominant charge carrier. However, it is known from the diffusion and transport number measurements quoted in Chapter II that the mobility of sodium ion vacancies is always higher than that of the chlorine ion vacancies in NaCl.

We are sure, however, that the observed Hall effect is not an electronic Hall effect. Electronic mobilities would be several orders of magnitude higher than our measured Hall mobility, and the temperature dependence of the electronic mobility would be opposite to that observed[51].

It is difficult to speculate about the source of our observed signal if we consider that source to be something other than the Hall effect. We are certain that the observed 25 cps signal was not produced in the apparatus exterior to the sample. Any spurious signal must have been produced by a source closely associated with the sample. The method of measurement which we have utilized automatically precludes observation of transverse effects other than the Hall effect, unless the temperature variations in the sample had large 60 or 85 cps components. This possibility is very unlikely.

As noted above, the most likely source of a spurious 25 cps signal is a nonlinear contact between a primary electrode and the sample. Induced 60 cps currents in the sample could conceivably coexist with the 85 cps primary current in these regions, and the mixing of the two currents in the nonlinear region could form a 25 cps signal. This signal would be proportional to the strength of the applied electric and magnetic fields but should be affected by the pressure exerted on the electrodes. Over the range of pressures used in our experiments the observed signals were not sensitive to the pressures applied. For this reason and since the Hall mobilities calculated from our data have the expected temperature dependence, we are fairly confident that the signals which we observed were in fact Hall voltages.

It is also difficult to speculate about the source of the noise which is associated with the 85 cps current. We are sure that the continuous noise is not created by either the vibration or the

plastic deformation of the sample. This noise could possibly be associated with the motion of electrons which are injected from the primary electrodes into the sample. Such injection might take place if the electrodes made contact with the sample over very small areas so that the potential gradient in this region was large. However, the observed noise level remained about the same although several types (platinum, silver, graphite) of electrode were used in the preliminary measurements. It is more likely that the noise is due to the fluctuation in the resistance of the sample-electrode contact at the primary electrodes.

Another possible source of the current noise might be associated with the formation of dislocations in the sample or the motion of internal subcrystalline boundaries. These processes might explain the observed burst noise.

In summary, we have observed a measurable change in the average level of the output of the Hall voltage system when the magnetic field is added to the electric field applied across the sample. For the reasons given above, we have attributed this increase in signal to the Hall effect. The Hall mobility calculated from our measured Hall voltage is in rough agreement with the sodium ion drift mobility measurements of Bean and of Etzel and Maurer.

The character of the current noise first observed by Levy has been further studied and possible sources eliminated. The source of the noise is closely related to the sample or the sample-electrode contact but is still unknown. There may be more than one noise source since the noise seems to take at least two definite forms.

3. Measurements in AgCl

Because of the uncertainties encountered in the Hall measurements on NaCl, we attempted to measure the ionic Hall effect in AgCl. It was hoped that the high level of current noise found in NaCl would not be present in AgCl. It was also hoped that the somewhat higher numerical difference in the carrier mobilities in AgCl would enhance the observed Hall signal. AgCl has the further advantage that the sample conductivity is higher by an order of magnitude than that of NaCl. The main problem in the use of AgCl is that it is a photoconductor and thus must be shielded from light if it is to remain a pure ionic conductor.

Several series of measurements were attempted on one sample of AgCl without success. This lack of success, however, was due to the imperfect light shielding of the sample rather than to an excess of current noise. The sample apparently absorbed a considerable amount of light during its preparation, for a large amount of photolytic silver was observed both on the face and in the bulk of the sample. The surface silver was deposited in the form of both large and small dendrites which were as long as 2 cm. The internally deposited silver was, under microscopic examination, found to be distributed along dislocation lines and networks, much in the manner observed by Hedges and Mitchell[57]. The presence of this photolytic silver was first detected by the erratic variations in the apparent sample conductivity at high temperatures. It was found that the silver formed a short

circuit across the primary electrodes. This short circuit existed even after the surface silver was washed away and made Hall measurements impossible.

It was not possible with our present equipment to make Hall measurements on AgCl. However, if a light-tight apparatus were used, the prospects for making a successful Hall measurement seem good since the current noise level (using Ag electrodes) was quite low compared to that of NaCl.

4. Suggestions for Future Measurements

In NaCl the major experimental problem is the high level of current noise. We have suggested that this noise may originate at the sample-electrode interfaces. We have also suggested that this same interface could possibly be the source of a spurious 25 cps signal. Thus it would seem desirable to eliminate the applied field electrodes.

A Hall effect measurement technique which utilizes an electric field which is not applied by means of electrodes has been suggested by Perrier[58] and elaborated by Pohl[59]. In this method the sample is cut in the shape of an annulus and an alternating magnetic field is applied in a direction perpendicular to the plane of the annulus. The magnetic field introduces an alternating electric field in the annulus of the same frequency as the magnetic field. This electric field will be directed circularly around the annulus. The charge carriers in the annulus are subject to both the electric

and magnetic fields and will be forced toward the inside or the outside of the annulus. The resulting charge distribution will create a potential between the inside and outside surfaces of the annulus. This Hall potential will appear at the sum and difference frequencies which will be twice the frequency of the magnetic field and zero respectively. The ac component of the Hall voltage is measured in order to retain the advantages of the ac method.

This method has the additional advantage that the magnitude of the induced electric field can, within limits, be raised by increasing the frequency of the applied magnetic field. Also, the shorting effects of the primary electrodes are eliminated so that the full Hall voltage appears across the sample. It may be possible to use this method to make Hall measurements on NaCl and AgCl at high temperatures. If the elimination of the primary electrodes led to a significant lowering of the current noise level, it should be possible to make much more accurate Hall measurements. It might be possible to measure the phase of the observed Hall signal (using a phase-sensitive detector) and thereby determine the sign of the dominant charge carrier. It might also be possible to resolve the mobilities of the two types of ionic charge carriers in these materials.

Further Hall measurements on AgCl require, in addition, the development of a light-tight Hall apparatus. It might also be of interest to attempt Hall measurements in AgCl using the more conventional electrode configuration.

In any case, successful Hall measurements using these refined techniques would represent an additional verification that the effect which we have measured in our experiments is the Hall effect.

BIBLIOGRAPHY

1. N. F. Mott and R. W. Gurney, Electronic Processes in Ionic Crystals (2nd ed., Oxford Univ. Press, London, 1948), Chapter II.

2. J. L. Levy, Thesis, University of Michigan, 1953.

3. J. L. Levy, Phys. Rev. 92, 215 (1953).

4. R. J. Friauf, "Ionic Conductivity in Solid Salts," American Institute of Physics Handbook, ed. D. E. Gray (McGraw-Hill, New York, 1957), pp. 5-185ff.

5. F. Bloch, Z. Physik 52, 555 (1928).

6. A. H. Wilson, The Theory of Metals (2nd ed., Cambridge Univ. Press, London, 1954), Chapter I.

7. A. B. Lidiard, "Ionic Conductivity," Handbuch der Physik, ed. S. Flügge (Springer-Verlag, Berlin, 1957), Vol. 20, pp. 246ff.

8. N. F. Mott and M. J. Littleton, Trans. Faraday Soc. 34, 485 (1938).

9. R. Guccione, M. P. Tosi, and M. Asdente, J. Phys. Chem. Solids 10, 162 (1959).

10. A. Ioffe, Ann. Physik 72, 461 (1923).

11. J. Frenkel, Z. Physik 35, 652 (1926).

12. W. Schottky, Z. physik. Chem. B29, 335 (1935).

13. E. Koch and C. Wagner, Z. physik. Chem. B38, 295 (1937).

14. R. Frerichs and I. Liberman, Phys. Rev. Letters 3, 215 (1959).

15. C. P. Bean, Thesis, University of Illinois, 1952.

16. K. Zückler, Thesis, Göttingen University, 1949.

17. H. W. Etzel and R. J. Maurer, J. Chem. Phys. 18, 1003 (1950).

18. H. Pick and H. Weber, Z. Physik 128, 409 (1950).

19. H. Kelting and H. Witt, Z. Physik 126, 697 (1949).

20. O. Stasiw and J. Teltow, Ann. Physik (6th series) 1, 261 (1947).

21. A. H. Wilson, The Theory of Metals (2nd ed., Cambridge Univ. Press, London, 1954), Chapter V.

22. F. Seitz, The Modern Theory of Solids (McGraw-Hill, New York, 1940), Chapter I.

23. C. Tubandt, H. Reinhold, and G. Liebold, Z. anorg. u. allgem. Chem. 197, 225 (1931).

24. W. Lehfeldt, Z. Physik 85, 717 (1933).

25. F. Kerkhoff, Z. Physik 130, 449 (1951).

26. F. Seitz, The Modern Theory of Solids (McGraw-Hill, New York, 1940), Chapter XV.

27. H. B. Huntington, Phys. Rev. 91, 1092 (1953).

28. W. D. Compton, Phys. Rev. 101, 1209 (1956).

29. I. Ebert and J. Teltow, Ann. Physik (6th series) 15, 268 (1955).

30. C. Wert, Phys. Rev. 79, 601 (1950).

31. G. J. Dienes, Phys. Rev. 89, 185 (1953).

32. G. H. Vineyard and G. J. Dienes, Phys. Rev. 93, 265 (1954).

33. S. A. Rice, Phys. Rev. 112, 804 (1958).

34. N. F. Mott and R. W. Gurney, Electronic Processes in Ionic Crystals (2nd ed., Oxford Univ. Press, London, 1948), Chapter III.

35. F. Seitz, Revs. Modern Phys. 18, 384 (1946).

36. H. Dorendorf and H. Pick, Z. Physik 128, 166 (1950).

37. A. B. Lidiard, Phys. Rev. 94, 29 (1954).

38. A. Smekal, "Strukturempfindliche Eigenschaften der Kristalle," Handbuch der Physik, ed. H. Geiger and K. Scheel (Springer, Berlin, 1933), Vol. 24, Part 2, p. 882.

39. D. Mapother, H. N. Crooks, and R. J. Maurer, J. Chem. Phys. 18, 1231 (1950).

40. T. E. Phipps, W. D. Lansing, and T. G. Cooke, J. Am. Chem. Soc. 48, 112 (1926).

41. F. Reif, Phys. Rev. 100, 1597 (1955).

42. A. S. Nowick and R. W. Dreyfus, Bull. Am. Phys. Soc., Ser. II, 5, 200 (1960).

43. J. S. Dryden and R. J. Meakins, Discussions Faraday Soc. 23, 39 (1957).

44. J. Laurent and J. Benard, J. Phys. Chem. Solids 3, 7 (1957).

45. L. W. Barr, I. M. Hoodless, J. A. Morrison, and R. Rudham, Trans. Faraday Soc. 56, 697 (1960).

46. A. J. Dekker, Solid State Physics (Prentice Hall, Englewood Cliffs, N. J., 1957), p. 328.

47. W. Shockley, Electrons and Holes in Semiconductors (Van Nostrand, New York, 1950), p. 209.

48. D. Halliday, Introductory Nuclear Physics (2nd ed., Wiley, New York, 1955), p. 68.

49. I. Isenberg, B. R. Russel, and R. F. Greene, Rev. Sci. Instr. 19, 685 (1948).

50. B. R. Russel and C. Wahlig, Rev. Sci. Instr. 21, 1028 (1950).

51. A. H. Wilson, The Theory of Metals (2nd ed., Cambridge Univ. Press, London, 1954), Chapter VIII.

52. P. L. Read, Rev. Sci. Instr. (to be published).

53. V. H. Attree, Electronic Eng. 21, 100 (1949).

54. R. P. Sallen and E. L. Key, IRE Trans. Circuit Theory CT-2, 74 (1955).

55. R. G. Wylie, J. Sci. Instr. 31, 382 (1954).

56. G. E. Valley and H. Wallman, Vacuum Tube Amplifiers (MIT Radiation Lab. Series, Vol. 18; McGraw-Hill, New York, 1948), pp. 436ff.

57. J. M. Hedges and J. W. Mitchell, Phil. Mag. 44, 223 (1953).

58. A. L. Perrier, Helv. Phys. Acta. 24, 637 (1951).

59. R. G. Pohl, Rev. Sci. Instr. 30, 783 (1959).